

QCD and relativistic $O(\alpha_s v^2)$ corrections to hadronic decays of spin-singlet heavy quarkonia h_c , h_b and η_b

Jin-Zhao Li*

*Department of Physics and State Key Laboratory of Nuclear Physics and Technology, Peking University, Beijing 100871, China*Yan-Qing Ma[†]*Physics Department, Brookhaven National Laboratory, Upton, New York 11973, USA*Kuang-Ta Chao[‡]*Department of Physics and State Key Laboratory of Nuclear Physics and Technology, and Center for High Energy Physics, Peking University, Beijing 100871, China*

(Received 5 October 2012; published 2 August 2013)

We calculate the annihilation decay widths of spin-singlet heavy quarkonia h_c , h_b and η_b into light hadrons with both QCD and relativistic corrections at order $O(\alpha_s v^2)$ in nonrelativistic QCD. With appropriate estimates for the long-distance matrix elements by using the potential model and operator evolution method, we find that our predictions of these decay widths are consistent with recent experimental measurements. We also find that the $O(\alpha_s v^2)$ corrections are small for $b\bar{b}$ states but substantial for $c\bar{c}$ states. In particular, the negative contribution of $O(\alpha_s v^2)$ correction to the h_c decay can lower the decay width, as compared with previous predictions without the $O(\alpha_s v^2)$ correction, and thus result in a good agreement with the recent BESIII measurement.

DOI: [10.1103/PhysRevD.88.034002](https://doi.org/10.1103/PhysRevD.88.034002)

PACS numbers: 12.38.Bx, 13.25.Gv, 14.40.Pq

I. INTRODUCTION

The inclusive annihilation decay of heavy quarkonium is one of the important issues in heavy quarkonium physics. It is widely accepted that the heavy quarkonium inclusive annihilation decay can be described by nonrelativistic QCD (NRQCD) factorization [1]. In this framework, the long-distance effects that cannot be calculated perturbatively are described by the long-distance matrix elements (LDMEs), which are classified in the order of v , the relative velocity of heavy quarks in quarkonium. As v is small in the heavy quarkonium system, we need to keep only a finite number of LDMEs in the calculation. Recently, more precise measurements for heavy quarkonium decay widths and branching ratios became available [2–12]. Thus, it is necessary to provide more precise theoretical predictions to compare with the data.

For charmonium, the $c\bar{c}$ system, the inclusive annihilation hadronic decay (into gluons and light quark pairs) widths for S -, P -, and D -wave states are all calculated up to $O(\alpha_s)$ in NRQCD [13–19]. Particularly, for the S -wave state η_c , the $O(\alpha_s v^2)$ corrections have recently been carried out [20], which means the short-distance coefficients of $O(v^2)$ LDMEs are calculated perturbatively to next-to-leading order (NLO) in α_s . After taking the $O(\alpha_s v^2)$ corrections into account, the measurements of η_c decay can be described much better in NRQCD. For the P -wave state h_c , the earlier theoretical result at $O(\alpha_s)$ predicts the hadronic decay width

of h_c to be about 0.72 MeV [17], which is a factor of 2 larger than the latest measurements by BESIII, where the central value of the total width is about 0.73 MeV and the hadronic decay branching ratio is about 50% [5]. Thus it is necessary to study higher order in v corrections to examine whether the gap between theoretical predictions and experimental measurements can be explained. It will be an interesting test for the validity of NRQCD factorization for the charmonium system.

For bottomonium, the $b\bar{b}$ system, the value of v^2 is about 0.1, which is much smaller than $v^2 \approx 0.3$ for charmonium. It is then expected that the v^2 expansion should be better for bottomonium, thus the study of bottomonium is more solid to check NRQCD factorization. Recently, the process $h_b(1P) \rightarrow \eta_b(1S)\gamma$ was measured by the Belle Collaboration [8]. It was found that the η_b decay width was about 12.4 MeV, and the decay branching fraction of $\mathcal{B}[h_b(1P) \rightarrow \eta_b(1S)\gamma] = 49.2 \pm 5.7_{-3.3}^{+5.6}\%$. It is tempting to try to explain these data in NRQCD.

In this paper, we will perform the $O(\alpha_s v^2)$ calculations for the spin-singlet P -wave charmonium h_c and bottomonium h_b , and also for the spin-singlet S -wave bottomonium η_b . We find these corrections are important to understand the measured data. The rest of this paper is organized as follows. In Sec. II we briefly introduce the NRQCD factorization formalism in heavy quarkonium annihilation decays. Then we describe some technical method in calculating $O(\alpha_s v^2)$ short-distance coefficients in Sec. III. The results for S -wave and P -wave states including real and virtual contributions are presented in Sec. IV. With these results and appropriate estimates of the LDMEs, we

*lijinzhao86@gmail.com

[†]yqma@bnl.gov[‡]ktchao@pku.edu.cn

discuss the related phenomenology in Sec. V. In Appendix A, we calculate the evolution of LDMEs at $O(\alpha_s v^2)$. In Appendix B, we describe our factorization scheme choice and show how to eliminate higher twist operators. Finally, we give a brief summary in Sec. VI.

II. NRQCD FACTORIZATION FOR QUARKONIUM DECAY

In this section, we introduce the NRQCD factorization formula for the rates of spin-singlet heavy quarkonium ($\eta_{c,b}$ and $h_{c,b}$) decays to light hadrons. The inclusive annihilation decay width of heavy quarkonium can be factorized by the following formula [1],

$$\Gamma(H) = \sum_n \frac{2 \text{Im} f_n(\mu_\Lambda)}{m_Q^{d_n-4}} \langle H | \mathcal{O}_n(\mu_\Lambda) | H \rangle, \quad (1)$$

where $\text{Im} f_n(\mu_\Lambda)$ is the short-distance (SD) coefficient that can be perturbatively calculated using the full QCD Lagrangian. The LDMEs $\langle H | \mathcal{O}_n(\mu_\Lambda) | H \rangle$ involve nonperturbative effects and are classified by the relative velocity v between Q and \bar{Q} , according to power counting in Refs. [1,21–24].

The NRQCD Lagrangian can be derived by integrating out the degrees of freedom of order m_Q , the mass of the heavy quark, from the QCD Lagrangian, which gives

$$\mathcal{L}_{\text{NRQCD}} = \mathcal{L}_{\text{light}} + \mathcal{L}_{\text{heavy}} + \delta \mathcal{L}. \quad (2)$$

The heavy part of the Lagrangian describes the motions of (anti-)heavy quark in spacetime and is given by

$$\mathcal{L}_{\text{heavy}} = \psi^\dagger \left(i D_t + \frac{\mathbf{D}^2}{2m_Q} \right) \psi + \chi^\dagger \left(i D_t - \frac{\mathbf{D}^2}{2m_Q} \right) \chi, \quad (3)$$

where $\psi(\chi)$ denotes the Pauli spinor field that annihilates (creates) a heavy (anti-)quark, and $D_t(\mathbf{D})$ is the time (space) component of the gauge-covariant derivative D^μ . The light piece of the Lagrangian reads

$$\mathcal{L}_{\text{light}} = -\frac{1}{2} \text{Tr} G^{\mu\nu} G_{\mu\nu} + \sum_{n_f} \bar{q} i \not{D} q, \quad (4)$$

where $G^{\mu\nu}$ is the gluon field strength tensor, q is the Dirac spinor field of light quarks, and n_f is the number of light flavors. The bilinear Lagrangian term which contains the order v^2 correction is

$$\begin{aligned} \delta \mathbf{L}_{\text{bilinear}} = & \frac{c_1}{8m_Q^3} \psi^\dagger (\mathbf{D}^2)^2 \psi + \frac{c_2}{8m_Q^2} \psi^\dagger (\mathbf{D} \cdot g\mathbf{E} - g\mathbf{E} \cdot \mathbf{D}) \psi \\ & + \frac{c_3}{8m_Q^2} \psi^\dagger (i\mathbf{D} \times g\mathbf{E} - g\mathbf{E} \times i\mathbf{D}) \cdot \boldsymbol{\sigma} \psi \\ & + \frac{c_4}{2m_Q} \psi^\dagger (g\mathbf{B} \cdot \boldsymbol{\sigma}) \psi + \text{charge conjugate terms}, \end{aligned} \quad (5)$$

where $E^i = G^{0i}$ and $B^i = \frac{1}{2} \epsilon^{ijk} G^{jk}$ are the electric and magnetic components of the gluon field strength tensor $G^{\mu\nu}$, and $c_i = 1 + O(\alpha_s)$, $i = 1, 2, 3, 4$ are the dimensionless coefficients corresponding to each operator.

In order to describe the annihilation decay of quarkonium, a set of local four-fermion operators \mathcal{O}_i which appear in Eq. (1) are needed. For example, the operator $\psi^\dagger \chi \chi^\dagger \psi$ can annihilate a $Q\bar{Q}$ pair in the $^1S_0^{[1]}$ configuration. In our case, for the $O(\alpha_s v^2)$ calculation of spin-singlet quarkonium decay, the power counting rules [1] give the following seven operators and LDMEs in Eq. (1): for S -wave quarkonium,

$$\mathcal{O}(^1S_0^{[1]}) = \psi^\dagger \chi \chi^\dagger \psi, \quad (6a)$$

$$\mathcal{P}(^1S_0^{[1]}) = \frac{1}{2} \psi^\dagger \chi \chi^\dagger \left(-\frac{i\vec{\mathbf{D}}}{2} \right)^2 \psi + \text{H.c.}, \quad (6b)$$

for P -wave quarkonium,

$$\mathcal{O}(^1S_0^{[8]}) = \psi^\dagger T^a \chi \chi^\dagger T^a \psi, \quad (7a)$$

$$\mathcal{P}(^1S_0^{[8]}) = \frac{1}{2} \psi^\dagger T^a \chi \chi^\dagger T^a \left(-\frac{i\vec{\mathbf{D}}}{2} \right)^2 \psi + \text{H.c.}, \quad (7b)$$

$$\mathcal{O}(^1P_1^{[1]}) = \psi^\dagger \left(-\frac{i\vec{\mathbf{D}}}{2} \right) \chi \cdot \chi^\dagger \left(-\frac{i\vec{\mathbf{D}}}{2} \right) \psi, \quad (7c)$$

$$\mathcal{P}(^1P_1^{[1]}) = \frac{1}{2} \psi^\dagger \left(-\frac{i\vec{\mathbf{D}}}{2} \right) \chi \cdot \chi^\dagger \left(-\frac{i\vec{\mathbf{D}}}{2} \right)^3 \psi + \text{H.c.}, \quad (7d)$$

$$\mathcal{T}_{1-8}(^1S_0, ^1P_1) = \frac{1}{2} \psi^\dagger g\mathbf{E} \chi \cdot \chi^\dagger \vec{\mathbf{D}} \psi + \text{H.c.}, \quad (7e)$$

and

$$\langle \mathcal{O}(^{2S+1}L_J^{[1,8]}) \rangle_H \equiv \langle H | \mathcal{O}(^{2S+1}L_J^{[1,8]}) | H \rangle, \quad (8a)$$

$$\langle \mathcal{P}(^{2S+1}L_J^{[1,8]}) \rangle_H \equiv \langle H | \mathcal{P}(^{2S+1}L_J^{[1,8]}) | H \rangle. \quad (8b)$$

Note that, choosing different power counting rules, one may get a different set of operators. For example, in the power counting rule of Ref. [24], m_Q and v are homogeneous, which gives that the chromomagnetic field $g\mathbf{B}$ scales as $(m_Q v)^2$. While that field scales as $m_Q^2 v^4$ in Ref. [1], which is further suppressed by v^2 . As a result, many operators considered in Ref. [24] disappear in our calculation, leaving the above seven. These seven matrix elements are all independent with each other, i.e. they cannot be eliminated by field redefinition or Poincare invariance [24].

Using the seven operators, we give the explicit form of Eq. (1) for 1S_0 and 1P_1 states,

$$\Gamma(H(^1S_0) \rightarrow \text{LH}) = \frac{F(^1S_0^{[1]})}{m_Q^2} \langle \mathcal{O}(^1S_0^{[1]}) \rangle_{^1S_0} + \frac{G(^1S_0^{[1]})}{m_Q^4} \langle \mathcal{P}(^1S_0^{[1]}) \rangle_{^1S_0}, \quad (9a)$$

$$\Gamma(H(^1P_1) \rightarrow \text{LH}) = \frac{F(^1S_0^{[8]})}{m_Q^2} \langle \mathcal{O}(^1S_0^{[8]}) \rangle_{^1P_1} + \frac{G(^1S_0^{[8]})}{m_Q^4} \langle \mathcal{P}(^1S_0^{[8]}) \rangle_{^1P_1} + \frac{F(^1P_1^{[1]})}{m_Q^4} \langle \mathcal{O}(^1P_1^{[1]}) \rangle_{^1P_1} + \frac{G(^1P_1^{[1]})}{m_Q^6} \langle \mathcal{P}(^1P_1^{[1]}) \rangle_{^1P_1}. \quad (9b)$$

Note that we omit a term of $\frac{T(^1S_0, ^1P_1)}{m_Q^5} \langle \mathcal{T}_{1-8}(^1S_0, ^1P_1) \rangle_{^1P_1}$ in Eq. (9b) to simplify our theoretical framework, although the LDME $\langle \mathcal{T}_{1-8}(^1S_0, ^1P_1) \rangle_{^1P_1}$ is of the same order in v as $\langle \mathcal{P}(^1P_1^{[1]}) \rangle_{^1P_1}$. There are two reasons that lead us to do this simplification. Numerically, this contribution is small, which is because $T(^1S_0, ^1P_1)$ vanishes at leading order (LO) in α_s due to the charge parity conservation. Theoretically, and more importantly, this contribution is finite, that is, no infrared (IR) poles are needed to cancel between this channel and the other four channels in Eq. (9b). It is then impossible to distinguish this finite contribution from the renormalization scheme or factorization scheme choice of other operators, such as $\langle \mathcal{O}(^1P_1^{[1]}) \rangle_{^1P_1}$ or $\langle \mathcal{O}(^1S_0^{[8]}) \rangle_{^1P_1}$. Therefore, by ignoring this operator in the hadronic decay width, it is equivalent that we choose a specific renormalization scheme or factorization scheme for other operators. In Appendix B, we will give an explicit definition of our factorization scheme to absorb the term $\frac{T(^1S_0, ^1P_1)}{m_Q^5} \langle \mathcal{T}_{1-8}(^1S_0, ^1P_1) \rangle_{^1P_1}$. Although our scheme is in principle distinguished from the $\overline{\text{MS}}$ scheme, as we will discuss in Appendix B, there is no difference between these two schemes for our purpose in this work. As a result, we will pretend to use the $\overline{\text{MS}}$ scheme in the following.

Through the above factorization formula, one can match full QCD with NRQCD to get the short-distance (SD) coefficients F and G perturbatively. The skeleton of the matching procedure is given by

$$\begin{aligned} & \text{Im} \mathcal{M}(Q\bar{Q} \rightarrow Q\bar{Q})|_{\text{pert QCD}} \\ &= \sum_n \frac{2 \text{Im} f_n(\mu_\Lambda)}{m_Q^{d_n-4}} \langle Q\bar{Q} | \mathcal{O}_n(\mu_\Lambda) | Q\bar{Q} \rangle |_{\text{NRQCD}}. \end{aligned} \quad (10)$$

The determination of SD coefficients will be discussed in detail in the next section.

III. DETAILS IN FULL QCD CALCULATION

A. Kinematics

We work in the rest frame of the heavy quarkonium. It is customary to decompose the momenta of Q and \bar{Q} as

$$p_Q = \frac{1}{2}P + q, \quad (11a)$$

$$p_{\bar{Q}} = \frac{1}{2}P - q, \quad (11b)$$

where P is the total momentum and q is half of the relative momentum, which satisfies the relation $P \cdot q = 0$. The explicit four-vector forms of P and q in the rest frame are

$$P = (2E_{\mathbf{q}}, \mathbf{0}), \quad (12a)$$

$$q = (0, \mathbf{q}), \quad (12b)$$

with $E_{\mathbf{q}} = \sqrt{m_Q^2 + \mathbf{q}^2}$.

The treatment of final state phase space integration at the $O(\alpha_s v^2)$ level is slightly different from ordinary calculations (i.e., leading order of v calculation). To make it simpler, we use the following rescaling transformation for all external momenta [20,25],

$$P \rightarrow P' \frac{E_{\mathbf{q}}}{m_Q}, \quad (13a)$$

$$k_f \rightarrow k'_f \frac{E_{\mathbf{q}}}{m_Q}, \quad (13b)$$

but keep the relative momentum q and loop integral momentum l unchanged. Once we take such a trick, the \mathbf{q}^2 dependence in both phase space and current factor [i.e., $1/(2M)$ where M is the quarkonium mass] can be absorbed into the amplitude, then we can safely take $\mathbf{q} \rightarrow 0$ in these terms and only expand \mathbf{q} , \mathbf{q}' at the amplitude level, where \mathbf{q}' is half of the relative momentum between the $Q\bar{Q}$ pair on the complex conjugate side. (Note that $|\mathbf{q}| = |\mathbf{q}'|$, but their direction does not need to be the same, so in general $\mathbf{q} \neq \mathbf{q}'$). It should be kept in mind that this trick can only work in the case where all final state partons are massless (i.e., gluons and light quarks), because, in the case of massive partons, the on-shell relation does not hold under rescaling, which will break the QCD gauge invariance.

B. Covariant projection method in D dimension

Instead of using the matching method directly, we use an equivalent but more efficient method, i.e., the covariant projection method, to calculate the imaginary part of the SD coefficients in Eqs. (9a) and (9b). In order to get spin-singlet $Q\bar{Q}$ decay amplitudes, we take the following spin and color projectors onto $Q\bar{Q}$ quark lines [26]:

$$\begin{aligned} \Pi_0 &= \frac{1}{2\sqrt{2}(E_{\mathbf{q}} + m_Q)} \left(\frac{\not{P}}{2} + \not{q} + m_Q \right) \\ &\times \frac{(\not{P} + 2E_{\mathbf{q}})\gamma_5(-\not{P} + 2E_{\mathbf{q}})}{8E_{\mathbf{q}}^2} \left(\frac{\not{P}}{2} - \not{q} - m_Q \right), \end{aligned} \quad (14)$$

and

$$C_1 = \frac{1}{\sqrt{N_c}}, \quad (15a)$$

$$C_8 = \sqrt{2}\mathbf{T}^a. \quad (15b)$$

We do Taylor expansion of the projected amplitudes in powers of q to the required order,

$$\begin{aligned} \mathcal{M}(q) = & \mathcal{M}(0) + \frac{\partial \mathcal{M}(q)}{\partial q^\alpha} \Big|_{q=0} q^\alpha + \frac{1}{2!} \frac{\partial^2 \mathcal{M}(q)}{\partial q^\alpha \partial q^\beta} \Big|_{q=0} q^\alpha q^\beta \\ & + \frac{1}{3!} \frac{\partial^3 \mathcal{M}(q)}{\partial q^\alpha \partial q^\beta \partial q^\gamma} \Big|_{q=0} q^\alpha q^\beta q^\gamma + \dots, \end{aligned} \quad (16)$$

and then make the replacement,

$$q_\alpha q_\beta \rightarrow \frac{\mathbf{q}^2}{D-1} \Pi_{\alpha\beta}, \quad (17a)$$

$$q_\alpha q'_\beta \rightarrow \frac{\mathbf{q} \cdot \mathbf{q}'}{D-1} \Pi_{\alpha\beta}, \quad (17b)$$

$$q_\alpha q_\beta q_\gamma q'_\lambda \rightarrow \frac{\mathbf{q}^2 \mathbf{q} \cdot \mathbf{q}'}{D+1} (\Pi_{\alpha\beta} \Pi_{\gamma\lambda} + \Pi_{\alpha\gamma} \Pi_{\beta\lambda} + \Pi_{\alpha\lambda} \Pi_{\gamma\beta}), \quad (17c)$$

to project them to definite states, where

$$\Pi_{\alpha\beta} = -g_{\alpha\beta} + \frac{P'_\alpha P'_\beta}{4m_Q^2}, \quad (18)$$

with P' the rescaled heavy quarkonium momentum. For example, the third derivative term of \mathcal{M} convolutes with the first derivative term of \mathcal{M}^\dagger , giving the squared amplitudes term,

$$\begin{aligned} & \frac{1}{3!} \frac{\partial^3 \mathcal{M}(q)}{\partial q^\alpha \partial q^\beta \partial q^\gamma} \Big|_{q=0} \frac{\partial \mathcal{M}^\dagger(q')}{\partial q'^\lambda} \Big|_{q'=0} q^\alpha q^\beta q^\gamma q'^\lambda \\ & \rightarrow \frac{1}{3!} \frac{\mathbf{q}^2 \mathbf{q} \cdot \mathbf{q}'}{D+1} (\Pi_{\alpha\beta} \Pi_{\gamma\lambda} + \Pi_{\alpha\gamma} \Pi_{\beta\lambda} + \Pi_{\alpha\lambda} \Pi_{\gamma\beta}) \\ & \times \frac{\partial^3 \mathcal{M}(q)}{\partial q^\alpha \partial q^\beta \partial q^\gamma} \Big|_{q=0} \frac{\partial \mathcal{M}^\dagger(q')}{\partial q'^\lambda} \Big|_{q'=0}, \end{aligned} \quad (19)$$

which contributes to the SD coefficient of $G(^1P_1^{[1]})$ in Eq. (9b).

IV. PERTURBATIVE QCD RESULTS OF SHORT-DISTANCE COEFFICIENTS

We generate Feynman diagrams and amplitudes by FEYNARTS [27,28], and then calculate the squared amplitudes by self-written MATHEMATICA codes. The phase space integrals are done analytically using the method presented in Ref. [16]. Ultraviolet (UV) and IR divergences are both regularized by dimensional regularization. The renormalizations for heavy quark mass m_Q , heavy quark field ψ_Q , light quark field ψ_q , and gluon field A_μ are in the on-mass-shell scheme (OS), and that for the QCD coupling constant g_s is in the $\overline{\text{MS}}$ scheme,

$$\delta Z_{m_Q}^{\text{OS}} = -3C_F \frac{\alpha_s}{4\pi} N_\epsilon \left[\frac{1}{\epsilon_{\text{UV}}} + \frac{4}{3} \right], \quad (20a)$$

$$\delta Z_2^{\text{OS}} = -C_F \frac{\alpha_s}{4\pi} N_\epsilon \left[\frac{1}{\epsilon_{\text{UV}}} + \frac{2}{\epsilon_{\text{IR}}} + 4 \right], \quad (20b)$$

$$\delta Z_{2l}^{\text{OS}} = -C_F \frac{\alpha_s}{4\pi} N_\epsilon \left[\frac{1}{\epsilon_{\text{UV}}} - \frac{1}{\epsilon_{\text{IR}}} \right], \quad (20c)$$

$$\delta Z_3^{\text{OS}} = \frac{\alpha_s}{4\pi} N_\epsilon \left[(\beta_0 - 2C_A) \left(\frac{1}{\epsilon_{\text{UV}}} - \frac{1}{\epsilon_{\text{IR}}} \right) \right], \quad (20d)$$

$$\delta Z_g^{\overline{\text{MS}}} = -\frac{\beta_0}{2} \frac{\alpha_s}{4\pi} N_\epsilon \left[\frac{1}{\epsilon_{\text{UV}}} + \ln \frac{m_Q^2}{\mu_r^2} \right], \quad (20e)$$

where $N_\epsilon(m_Q) = \left(\frac{4\pi\mu_r^2}{m_Q^2} \right)^\epsilon \Gamma(1+\epsilon)$ is an overall factor, and μ_r is the renormalization scale. $\beta_0 = \frac{11}{3}C_A - \frac{4}{3}T_F n_f$ is the one-loop coefficient of the β function, n_f is the active quark flavors, which we set to be 3 for charmonium and 4 for bottomonium.

A. Short-distance coefficients of S-wave quarkonium hadronic decay

Leading order in α_s calculations give the Born-level decay width and its relativistic correction, respectively, as

$$\begin{aligned} \Gamma_{\text{Born}}(^1S_0^{[1]} \rightarrow gg) = & \frac{4}{3} (4\pi\alpha_s)^2 \frac{\mu_r^{4\epsilon}}{m_Q^2} \Phi_{(2)}(1-\epsilon)(1-2\epsilon) \\ & \times \frac{\langle \mathcal{O}(^1S_0^{[1]}) \rangle_{1S_0}^{\text{Born}}}{2N_c}, \end{aligned} \quad (21a)$$

$$\Gamma_{\text{Born}}^{(v^2)}(^1S_0^{[1]} \rightarrow gg) = -\frac{2(2-\epsilon)}{3-2\epsilon} \frac{\mathbf{q}^2}{m_Q^2} \Gamma_{\text{Born}}(^1S_0^{[1]} \rightarrow gg), \quad (21b)$$

where $\Phi_{(2)} = \frac{1}{8\pi} \left(\frac{4\pi}{M^2} \right)^\epsilon \frac{\Gamma(1-\epsilon)}{\Gamma(2-2\epsilon)}$ is the total two-body phase space in D dimension, and $M = 2m_Q \sqrt{1 + \frac{\mathbf{q}^2}{m_Q^2}}$ is the quarkonium mass including the relativistic correction. The two Born diagrams are illustrated in Fig. 1.

The next-to-leading order calculations include real and virtual corrections. For S-wave Fock states (i.e., $^1S_0^{[1]}$ and $^1S_0^{[8]}$), UV divergences will be canceled by counterterm diagrams, and most IR divergences will be canceled between real and virtual corrections, leaving some residue divergences at $O(v^2)$. The cancellation of such residue divergences will be presented in the next section by calculating NRQCD LDMEs at the one-loop level. The contribution of virtual plus counterterm corrections is

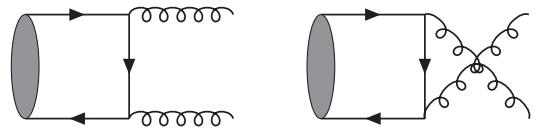


FIG. 1. Born-level Feynman diagrams for $^1S_0^{[1]}, ^1S_0^{[8]} \rightarrow gg$.

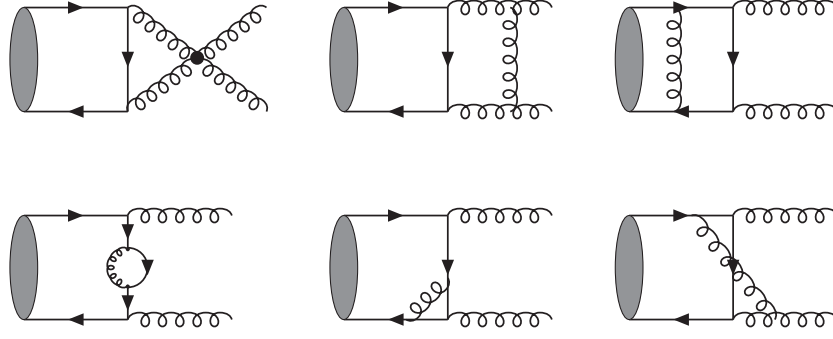


FIG. 2. Virtual correction Feynman diagrams for $^1S_0^{[1]}, ^1S_0^{[8]} \rightarrow gg$. The crossed diagrams have been suppressed.

$$\Gamma_{\text{Virtual}}(^1S_0^{[1]} \rightarrow gg) = \frac{3\alpha_s}{\pi} \Gamma_{\text{Born}}(^1S_0^{[1]} \rightarrow gg) f_\epsilon(m_Q) \left\{ \left[-\frac{1}{\epsilon^2} - \frac{1}{6} \beta_0 \frac{1}{\epsilon} + \frac{1}{36} \left(-6\beta_0 \ln\left(\frac{4m_Q^2}{\mu_r^2}\right) + 19\pi^2 - 44 \right) \right] \right. \\ \left. + \frac{\mathbf{q}^2}{m_Q^2} \left[\frac{4}{3} \frac{1}{\epsilon^2} - \frac{4n_f - 97}{27} \frac{1}{\epsilon} - \frac{1}{324} \left(-72\beta_0 \ln\left(\frac{4m_Q^2}{\mu_r^2}\right) + 8n_f + 267\pi^2 - 280 \right) \right] \right\}, \quad (22)$$

where $f_\epsilon(m_Q) = \left(\frac{\pi\mu_r^2}{m_Q^2}\right)^\epsilon \Gamma(1 + \epsilon)$. Some selected Feynman diagrams are shown in Fig. 2.

The real correction contains two sets, where one set is the final states with ggg and the other one with $q\bar{q}g$. Some typical Feynman diagrams are shown in Fig. 3 and 4 and the contributions to decay width are

$$\Gamma(^1S_0^{[1]} \rightarrow ggg) = \frac{3\alpha_s}{\pi} \Gamma_{\text{Born}}(^1S_0^{[1]} \rightarrow gg) f_\epsilon(m_Q) \left\{ \left[\frac{1}{\epsilon^2} + \frac{11}{6} \frac{1}{\epsilon} + \frac{1}{72} (724 - 69\pi^2) \right] + \frac{\mathbf{q}^2}{m_Q^2} \left[-\frac{4}{3} \frac{1}{\epsilon^2} - \frac{3}{\epsilon} - \frac{437 - 42\pi^2}{27} \right] \right\}, \quad (23a)$$

$$\Gamma(^1S_0^{[1]} \rightarrow q\bar{q}g) = \frac{n_f \alpha_s}{2\pi} \Gamma_{\text{Born}}(^1S_0^{[1]} \rightarrow gg) \frac{f_\epsilon(m_Q)}{\Gamma(1 + \epsilon)\Gamma(1 - \epsilon)} \left[-\frac{2}{3} \frac{1}{\epsilon} - \frac{16}{9} + \frac{\mathbf{q}^2}{m_Q^2} \left(\frac{8}{9} \frac{1}{\epsilon} + \frac{86}{27} \right) \right]. \quad (23b)$$

Combining Eqs. (21)–(23), we obtain the hadronic decay width with both QCD radiative and relativistic corrections at NLO of 1S_0 heavy quarkonium,

$$\Gamma_{\text{QCD}}(^1S_0 \rightarrow \text{LH}) = \Gamma_{\text{Born}}(^1S_0^{[1]} \rightarrow gg) \left\{ \left[1 + \frac{\alpha_s}{\pi} f_\epsilon(m_Q) \frac{1}{72} \left(-36\beta_0 \ln\left(\frac{4m_Q^2}{\mu_r^2}\right) - 64n_f - 93\pi^2 + 1908 \right) \right] \right. \\ \left. - \frac{4}{3} \frac{\mathbf{q}^2}{m_Q^2} \left[1 + \frac{\alpha_s}{\pi} f_\epsilon(m_Q) \left(-\frac{4}{3} \frac{1}{\epsilon} + \frac{1}{144} \left(-72\beta_0 \ln\left(\frac{4m_Q^2}{\mu_r^2}\right) - 164n_f - 237\pi^2 + 4964 \right) \right) \right] \right\}. \quad (24)$$

We note that our results agree with the previous work for $O(\alpha_s v^2)$ correction [20] and $O(\alpha_s)$ correction [16,19]. Comparing our results with Ref. [20], a slight difference of two-body phase space Φ_2 between them can be found. In Ref. [20] Φ_2 is defined so as to remove the \mathbf{q}^2 dependence

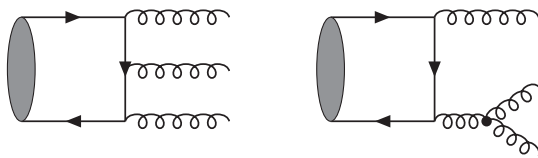


FIG. 3. Real correction Feynman diagrams for $^1S_0^{[1]}, ^1S_0^{[8]}, ^1P_1^{[1]} \rightarrow ggg$. The crossed diagrams have been suppressed. The second diagram vanishes in $^1P_1^{[1]}$.

into the coefficients, so our individual virtual and real parts, Eqs. (22) and (23), look different from the results in Ref. [20], but essentially they are equivalent. The total NLO result Eq. (24) is explicitly the same, independent of the definition of Φ_2 . The correct repetition of the hadronic decay SD coefficients of 1S_0 heavy quarkonium enables us

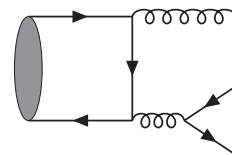


FIG. 4. Real correction Feynman diagrams for $^1S_0^{[1]}, ^1S_0^{[8]} \rightarrow q\bar{q}g$. The crossed diagrams have been suppressed.

to extend discussion from charm quark system to bottom quark system (i.e. η_b) and also partly checks our codes when dealing with P -wave heavy quarkonium.

B. Short-distance coefficients of P -wave quarkonium hadronic decay

The procedure in calculating the 1P_1 heavy quarkonium is similar to 1S_0 , although more complicated. Additional simplification can be taken by imposing C (charge) parity conservation of QCD to constrain Feynman diagrams. A straightforward result is that C parity conservation prohibits $^1P_1^{[1]}$ Fock state, which has $C = -1$, to decay to two gluons, whose $C = +1$, whether they are real or virtual.

By tedious but straightforward calculation, we get the results as follows.

At the Born level,

$$\Gamma_{\text{Born}}(^1S_0^{[8]} \rightarrow gg) = \frac{5}{12} (4\pi\alpha_s)^2 \frac{\mu_r^{4\epsilon}}{m_Q^2} \Phi_{(2)}(1-\epsilon)(1-2\epsilon) \times \langle \mathcal{O}(^1S_0^{[8]})_{^1P_1} \rangle_{\text{Born}}, \quad (25a)$$

$$\Gamma_{\text{Born}}^{(v^2)}(^1S_0^{[8]} \rightarrow gg) = -\frac{2(2-\epsilon)}{3-2\epsilon} \frac{\mathbf{q}^2}{m_Q^2} \Gamma_{\text{Born}}(^1S_0^{[8]} \rightarrow gg). \quad (25b)$$

For NLO corrections,

$$\Gamma_{\text{Virtual}}(^1S_0^{[8]} \rightarrow gg) = \frac{3\alpha_s}{\pi} \Gamma_{\text{Born}}(^1S_0^{[8]} \rightarrow gg) f_\epsilon(m_Q) \left\{ \left[-\frac{1}{\epsilon^2} + \frac{n_f - 21}{9} \frac{1}{\epsilon} + \frac{1}{72} \left(-12\beta_0 \ln\left(\frac{4m_Q^2}{\mu_r^2}\right) + 29\pi^2 - 16 \right) \right] + \frac{\mathbf{q}^2}{m_Q^2} \left[\frac{4}{3} \frac{1}{\epsilon^2} - \frac{4n_f - 115}{27} \frac{1}{\epsilon} - \frac{1}{628} \left(-144\beta_0 \ln\left(\frac{4m_Q^2}{\mu_r^2}\right) + 16n_f + 345\pi^2 - 992 \right) \right] \right\}, \quad (26)$$

$$\Gamma(^1S_0^{[8]} \rightarrow ggg) = \frac{3\alpha_s}{\pi} \Gamma_{\text{Born}}(^1S_0^{[8]} \rightarrow ggg) f_\epsilon(m_Q) \left\{ \left[\frac{1}{\epsilon^2} + \frac{7}{3} \frac{1}{\epsilon} - \pi^2 + \frac{104}{9} \right] + \frac{\mathbf{q}^2}{m_Q^2} \left[-\frac{4}{3} \frac{1}{\epsilon^2} - \frac{4}{\epsilon} - \frac{554 - 45\pi^2}{27} \right] \right\}, \quad (27)$$

$$\Gamma(^1S_0^{[8]} \rightarrow q\bar{q}g) = \frac{n_f}{2} \frac{\alpha_s}{\pi} \Gamma_{\text{Born}}(^1S_0^{[8]} \rightarrow gq\bar{q}) \frac{f_\epsilon(m_Q)}{\Gamma(1+\epsilon)\Gamma(1-\epsilon)} \left[-\frac{2}{3} \frac{1}{\epsilon} - \frac{16}{9} + \frac{\mathbf{q}^2}{m_Q^2} \left(\frac{8}{9} \frac{1}{\epsilon} + \frac{86}{27} \right) \right], \quad (28)$$

$$\Gamma(^1P_1^{[1]} \rightarrow ggg) = \frac{40\alpha_s^3}{27} f_\epsilon(m_Q) (8\pi\Phi_2) \left\{ \left[-\frac{1}{\epsilon} + \frac{7\pi^2}{24} - \frac{5}{3} \right] + \frac{\mathbf{q}^2}{m_Q^2} \left[\frac{29}{15} \frac{1}{\epsilon} + \frac{4216 - 555\pi^2}{900} \right] \right\} \frac{\langle \mathcal{O}(^1P_1^{[1]})_{^1P_1} \rangle_{\text{Born}}}{2N_c m_Q^4}. \quad (29)$$

Summing over the above results, we get the total hadronic decay width,

$$\Gamma_{\text{QCD}}(^1P_1 \rightarrow \text{LH}) = \Gamma_{\text{Born}}(^1S_0^{[8]} \rightarrow gg) \left\{ \left[1 + \frac{\alpha_s}{\pi} f_\epsilon(m_Q) \left(-\frac{1}{2} \beta_0 \ln\left(\frac{4m_Q^2}{\mu_r^2}\right) - \frac{8}{9} n_f - \frac{43\pi^2}{24} + 34 \right) \right] - \frac{4}{3} \frac{\mathbf{q}^2}{m_Q^2} \left[1 + \frac{\alpha_s}{\pi} f_\epsilon(m_Q) \left(-\frac{7}{12} \frac{1}{\epsilon} + \frac{1}{288} \left(-144\beta_0 \ln\left(\frac{4m_Q^2}{\mu_r^2}\right) - 328n_f - 735\pi^2 + 12304 \right) \right) \right] \right\} + \frac{40\alpha_s^3}{27} f_\epsilon(m_Q) (8\pi\Phi_2) \left\{ \left[-\frac{1}{\epsilon} + \frac{7\pi^2}{24} - \frac{5}{3} \right] + \frac{\mathbf{q}^2}{m_Q^2} \left[\frac{29}{15} \frac{1}{\epsilon} + \frac{4216 - 555\pi^2}{900} \right] \right\} \frac{\langle \mathcal{O}(^1P_1^{[1]})_{^1P_1} \rangle_{\text{Born}}}{2N_c m_Q^4}. \quad (30)$$

C. Evaluating NRQCD LDMEs and matching full QCD results

In Eqs. (24) and (30), there exist explicit IR divergences. To cancel these divergences, we need to evaluate LDMEs at the loop level. By replacing all the Born LDMEs appearing in Eqs. (24) and (30) by one-loop LDMEs, all IR divergences should be canceled and the final results will be infrared-safe quantities.

The self-energy contributions that connect Born LDMEs to their corresponding relativistic ones are first calculated in Ref. [1]. The intersecting diagrams that describe the E1 transition between $^1S_0^{[8]}$ and $^1P_1^{[1]}$ states at $\mathcal{O}(\alpha_s v^2)$ in this work are new. The detailed calculation is presented in Appendix A. Here we give the relevant results in dimensional regularization with $\overline{\text{MS}}$ renormalization scheme,

$$\langle \mathcal{O}(^1S_0^{[1]}) \rangle_{1S_0}^{\text{Bom}} \rightarrow \langle \mathcal{O}(^1S_0^{[1]}) \rangle_{1S_0}^{(\mu_\Lambda)} \left[1 - \frac{4}{3} \frac{\mathbf{q}^2}{m_Q^2} \frac{4\alpha_s}{3\pi} f_\epsilon(m_Q) \left[\frac{1}{\epsilon} - \ln \left(\frac{\mu_\Lambda^2}{4m_Q^2} \right) \right] \right], \quad (31a)$$

$$\begin{aligned} \langle \mathcal{O}(^1S_0^{[8]}) \rangle_{1P_1}^{\text{Bom}} &\rightarrow \langle \mathcal{O}(^1S_0^{[8]}) \rangle_{1P_1}^{(\mu_\Lambda)} \left[1 - \frac{4}{3} \frac{\mathbf{q}^2}{m_Q^2} \frac{7\alpha_s}{12\pi} f_\epsilon(m_Q) \left[\frac{1}{\epsilon} - \ln \left(\frac{\mu_\Lambda^2}{4m_Q^2} \right) \right] \right] + \frac{16\alpha_s}{9\pi} f_\epsilon(m_Q) \left\{ \left[\frac{1}{\epsilon} - \ln \left(\frac{\mu_\Lambda^2}{4m_Q^2} \right) \right] \right. \\ &\quad \left. + \frac{3\mathbf{q}^2}{5m_Q^2} \left[-\frac{1}{\epsilon} + \ln \left(\frac{\mu_\Lambda^2}{4m_Q^2} \right) \right] \right\} \frac{\langle \mathcal{O}(^1P_1^{[1]}) \rangle_{1P_1}^{\text{Bom}}}{2N_c m_Q^2}, \end{aligned} \quad (31b)$$

$$\langle \mathcal{P}(^1S_0^{[8]}) \rangle_{1P_1}^{\text{Bom}} \rightarrow \langle \mathcal{P}(^1S_0^{[8]}) \rangle_{1P_1}^{(\mu_\Lambda)} + \frac{16\alpha_s}{9\pi} f_\epsilon(m_Q) \left[\frac{1}{\epsilon} - \ln \left(\frac{\mu_\Lambda^2}{4m_Q^2} \right) \right] \frac{\langle \mathcal{P}(^1P_1^{[1]}) \rangle_{1P_1}^{\text{Bom}}}{2N_c m_Q^2}, \quad (31c)$$

where μ_Λ is the factorization scale. Substituting them into Eqs. (24) and (30), and considering the relation

$$\langle \mathcal{P}(^1S_0^{[1]}) \rangle_{1S_0}^{\text{Bom}} = \mathbf{q}^2 \langle \mathcal{O}(^1S_0^{[1]}) \rangle_{1S_0}^{\text{Bom}}, \quad (32a)$$

$$\langle \mathcal{P}(^1S_0^{[8]}) \rangle_{1P_1}^{\text{Bom}} = \mathbf{q}^2 \langle \mathcal{O}(^1S_0^{[8]}) \rangle_{1P_1}^{\text{Bom}}, \quad (32b)$$

$$\langle \mathcal{P}(^1P_1^{[1]}) \rangle_{1P_1}^{\text{Bom}} = \mathbf{q}^2 \langle \mathcal{O}(^1P_1^{[1]}) \rangle_{1P_1}^{\text{Bom}}, \quad (32c)$$

we get the SD coefficients for heavy quarkonium hadronic decay of S -wave and P -wave states by matching full QCD and NRQCD,

$$F(^1S_0^{[1]}) = \frac{4\pi\alpha_s^2}{9} \left[1 - \frac{\alpha_s}{\pi} \frac{1}{72} \left(36\beta_0 \ln \left(\frac{4m_Q^2}{\mu_r^2} \right) + 64n_f + 93\pi^2 - 1908 \right) \right], \quad (33a)$$

$$G(^1S_0^{[1]}) = -\frac{4}{3} \frac{4\pi\alpha_s^2}{9} \left\{ 1 - \frac{\alpha_s}{\pi} \frac{1}{144} \left[192 \ln \left(\frac{\mu_\Lambda^2}{4m_Q^2} \right) + 72\beta_0 \ln \left(\frac{4m_Q^2}{\mu_r^2} \right) + 164n_f + 237\pi^2 - 4964 \right] \right\}, \quad (33b)$$

$$F(^1S_0^{[8]}) = \frac{5\pi\alpha_s^2}{6} \left[1 - \frac{\alpha_s}{\pi} \frac{1}{72} \left(36\beta_0 \ln \left(\frac{4m_Q^2}{\mu_r^2} \right) + 64n_f + 129\pi^2 - 2448 \right) \right], \quad (33c)$$

$$G(^1S_0^{[8]}) = -\frac{4}{3} \frac{5\pi\alpha_s^2}{6} \left\{ 1 - \frac{\alpha_s}{\pi} \frac{1}{288} \left[168 \ln \left(\frac{\mu_\Lambda^2}{4m_Q^2} \right) + 144\beta_0 \ln \left(\frac{4m_Q^2}{\mu_r^2} \right) + 328n_f + 735\pi^2 - 12304 \right] \right\}, \quad (33d)$$

$$F(^1P_1^{[1]}) = \frac{5\alpha_s^3}{486} \left[7(\pi^2 - 16) - 24 \ln \left(\frac{\mu_\Lambda^2}{4m_Q^2} \right) \right], \quad (33e)$$

$$G(^1P_1^{[1]}) = \frac{\alpha_s^3}{3645} \left[1740 \ln \left(\frac{\mu_\Lambda^2}{4m_Q^2} \right) - 555\pi^2 + 9236 \right], \quad (33f)$$

where F 's and G 's are defined in Eqs. (9a) and (9b).

The SD coefficients of $^1S_0^{[1]}$ agree with those in Refs. [1,16,19,20,25], and that of $^1S_0^{[8]}$ and $^1P_1^{[1]}$ at leading order in v^2 also agree with the previous results in Ref. [16]. The relativistic corrections $G(^1S_0^{[8]})$ and $G(^1P_1^{[1]})$ are primarily new results in this work. Based on these results, we will analyze the decay of 1S_0 and 1P_1 heavy quarkonium into light hadrons.

V. PHENOMENOLOGICAL DISCUSSIONS

A. Estimating NRQCD LDMEs

To get the numerical result, we also need to know the value of LDMEs. For 1S_0 quarkonium there are two LDMEs, and for 1P_1 there are four. In Ref. [20] the LDMEs of η_c are determined by combining the Cornell

potential [29] with one experimental measurement, $\Gamma^{\text{LH}}(\eta_c)$ or $\Gamma^{\gamma\gamma}(\eta_c)$ [30], and then one can predict other quantities. In the present work, since there are not enough experimental inputs to determine all involved LDMEs, we will estimate them by other methods.

For η_b , the situation is similar to Ref. [20], but lacking the experimental input of the decay width to two photons $\Gamma^{\gamma\gamma}(\eta_b)$. In this case we will determine $\langle \mathcal{O}(^1S_0^{[1]}) \rangle_{\eta_b}$ from the potential model. Here we use the Buchmüller-Tye (B-T) potential model [31] and Cornell (Corn) potential model [29] results as input, which give [32,33]

$$\langle \mathcal{O}(^1S_0^{[1]}) \rangle_{\eta_b}^{\text{B-T}} = \frac{N_c}{2\pi} |R_S^{\text{B-T}}(0)|^2 = 3.093 \text{ GeV}^3, \quad (34a)$$

$$\langle \mathcal{O}(^1S_0^{[1]}) \rangle_{\eta_b}^{\text{Corn}} = \langle \mathcal{O}(^3S_1^{[1]}) \rangle_{Y(1S)}^{\text{Corn}} = 3.07_{-0.19}^{+0.21} \text{ GeV}^3. \quad (34b)$$

In Eq. (34b) we use the heavy quark spin symmetry (HQSS) to relate LDMEs of η_b with that of $Y(1S)$. As the B-T model and Cornell model give almost the same result, we will only use the B-T model in the following.

In order to determine $\langle \mathcal{P}(^1S_0^{[1]}) \rangle_{\eta_b}$, we define [20,25]

$$\langle \mathbf{v}^2 \rangle_{\eta_b} \equiv \frac{\langle \mathcal{P}(^1S_0^{[1]}) \rangle_{\eta_b}}{m_b^2 \langle \mathcal{O}(^1S_0^{[1]}) \rangle_{\eta_b}}. \quad (35)$$

Although $\langle \mathbf{v}^2 \rangle_{\eta_b}$ cannot be understood as the expectation value of \mathbf{v}^2 in the potential model, it can be estimated from the Gremm-Kapustin relation [34]

$$\langle \mathbf{v}^2 \rangle_{\eta_b}^{\text{G-K}} = \frac{m_{\eta_b} - 2m_{\text{pole}}}{m_{\text{pole}}}. \quad (36)$$

Choosing $m_{\text{pole}} = 4.6$ GeV for b quark and $m_{\eta_b} = 9.391$ GeV [30], we get $\langle \mathbf{v}^2 \rangle_{\eta_b} = 0.042$, which is close to the potential model estimated value $\mathbf{v}^2 \sim 0.05\text{--}0.1$. Combining these results, we get the value of redefined LDMEs in the B-T model as

$$\begin{aligned} \langle \bar{\mathcal{O}}(^1S_0^{[1]}) \rangle_{\eta_b} &\equiv \frac{\langle \mathcal{O}(^1S_0^{[1]}) \rangle_{\eta_b}}{2N_c m_b^2} = 24.36_{-1.03}^{+1.09} \text{ MeV}, \\ \langle \bar{\mathcal{P}}(^1S_0^{[1]}) \rangle_{\eta_b} &\equiv \frac{\langle \mathcal{P}(^1S_0^{[1]}) \rangle_{\eta_b}}{2N_c m_b^4} = \langle \mathbf{v}^2 \rangle_{\eta_b} \langle \bar{\mathcal{O}}(^1S_0^{[1]}) \rangle_{\eta_b} \\ &= 1.01_{-0.04}^{+0.05} \text{ MeV}, \end{aligned} \quad (37)$$

where the uncertainties are introduced by choosing $m_b = 4.6 \pm 0.1$ GeV.

For h_c , we need to determine four LDMEs $\langle \mathcal{O}(^1P_1^{[1]}) \rangle_{h_c}$, $\langle \mathcal{O}(^1S_0^{[8]}) \rangle_{h_c}$, $\langle \mathcal{P}(^1P_1^{[1]}) \rangle_{h_c}$, and $\langle \mathcal{P}(^1S_0^{[8]}) \rangle_{h_c}$. $\langle \mathcal{O}(^1P_1^{[1]}) \rangle_{h_c}$ is determined by the B-T potential model [32] and

$$\langle \mathcal{P}(^1P_1^{[1]}) \rangle_{h_c} \equiv \langle \mathbf{v}^2 \rangle_{h_c} m_c^2 \langle \mathcal{O}(^1P_1^{[1]}) \rangle_{h_c} \approx \langle \mathbf{v}^2 \rangle_{\eta_c} m_c^2 \langle \mathcal{O}(^1P_1^{[1]}) \rangle_{h_c}, \quad (38)$$

where $\langle \mathbf{v}^2 \rangle_{\eta_c} = 0.228$ is taken from Ref. [20]. Here we have tentatively assumed $\langle \mathbf{v}^2 \rangle_{h_c} \approx \langle \mathbf{v}^2 \rangle_{\eta_c}$. The remaining two-color octet LDMEs are determined by the operator evolution method (OEM) [1,34,35]. From Eq. (A10) we get the evolution equations,

$$\begin{aligned} \mu_\Lambda^2 \frac{d\langle \mathcal{O}(^1S_0^{[8]}) \rangle}{d\mu_\Lambda^2} &= -\frac{7\alpha_s}{9\pi} \frac{\langle \mathcal{P}(^1S_0^{[8]}) \rangle}{m_Q^2} + \frac{16\alpha_s}{9\pi} \frac{\langle \mathcal{O}(^1P_1^{[1]}) \rangle}{2N_c m_Q^2} \\ &\quad - \frac{16\alpha_s}{15\pi} \frac{\langle \mathcal{P}(^1P_1^{[1]}) \rangle}{2N_c m_Q^4}, \\ \mu_\Lambda^2 \frac{d\langle \mathcal{P}(^1S_0^{[8]}) \rangle}{d\mu_\Lambda^2} &= \frac{16\alpha_s}{9\pi} \frac{\langle \mathcal{P}(^1P_1^{[1]}) \rangle}{2N_c m_Q^2}. \end{aligned} \quad (39)$$

Knowing the values of $\langle \mathcal{O}(^1P_1^{[1]}) \rangle$ and $\langle \mathcal{P}(^1P_1^{[1]}) \rangle$, the above differential equations will determine the values of

$\langle \mathcal{O}(^1S_0^{[8]}) \rangle$ and $\langle \mathcal{P}(^1S_0^{[8]}) \rangle$ by evolving from initial values at $\mu_\Lambda = \mu_{\Lambda_0}$. Using the two-loop running of α_s , we get

$$\begin{aligned} \langle \mathcal{O}(^1S_0^{[8]}) \rangle^{(\mu_\Lambda)} &= \frac{64}{9\beta_0} A \frac{\langle \mathcal{O}(^1P_1^{[1]}) \rangle}{2N_c m_Q^2} - \frac{64}{3\beta_0} A \left(\frac{1}{5} + \frac{14}{27\beta_0} A \right) \\ &\quad \times \frac{\langle \mathcal{P}(^1P_1^{[1]}) \rangle}{2N_c m_Q^4} - \frac{28}{9\beta_0} A \frac{\langle \mathcal{P}(^1S_0^{[8]}) \rangle^{(\mu_{\Lambda_0})}}{m_Q^2} \\ &\quad + \langle \mathcal{O}(^1S_0^{[8]}) \rangle^{(\mu_{\Lambda_0})}, \\ \langle \mathcal{P}(^1S_0^{[8]}) \rangle^{(\mu_\Lambda)} &= \frac{64}{9\beta_0} A \frac{\langle \mathcal{P}(^1P_1^{[1]}) \rangle}{2N_c m_Q^2} + \langle \mathcal{P}(^1S_0^{[8]}) \rangle^{(\mu_{\Lambda_0})}, \end{aligned} \quad (40)$$

where $A \equiv \ln \frac{\alpha_s(\mu_{\Lambda_0})}{\alpha_s(\mu_\Lambda)} - \ln \frac{1+\alpha_s(\mu_{\Lambda_0})\beta_1/\beta_0}{1+\alpha_s(\mu_\Lambda)\beta_1/\beta_0}$ with $\beta_1 = (17C_A^2 - n_f T_R (10C_A + 6C_F)) / (6\pi)$. Choosing $\mu_{\Lambda_0} = m_c v \sim 0.8 \pm 0.2$ GeV, the OEM assumes that the values of $\langle \mathcal{O}(^1S_0^{[8]}) \rangle$ and $\langle \mathcal{P}(^1S_0^{[8]}) \rangle$ evaluated at $\mu_\Lambda \approx 2m_c$ can be estimated by the evolution term only, i.e., neglecting initial values at μ_{Λ_0} . Setting m_c to be its pole mass, 1.5 ± 0.1 GeV, LDMEs at $\mu_\Lambda = 2m_c$ are

$$\begin{aligned} \langle \bar{\mathcal{O}}(^1P_1^{[1]}) \rangle_{h_c} &\equiv \frac{\langle \mathcal{O}(^1P_1^{[1]}) \rangle_{h_c}}{2N_c m_c^4} = 3.537_{-0.805}^{+1.124} \text{ MeV}, \\ \langle \bar{\mathcal{P}}(^1P_1^{[1]}) \rangle_{h_c} &\equiv \frac{\langle \mathcal{P}(^1P_1^{[1]}) \rangle_{h_c}}{2N_c m_c^6} = 0.806_{-0.183}^{+0.256} \text{ MeV}, \\ \langle \bar{\mathcal{O}}(^1S_0^{[8]}) \rangle_{h_c} &\equiv \frac{\langle \mathcal{O}(^1S_0^{[8]}) \rangle_{h_c}}{m_c^2} = 2.040_{-0.704}^{+1.208} \text{ MeV}, \\ \langle \bar{\mathcal{P}}(^1S_0^{[8]}) \rangle_{h_c} &\equiv \frac{\langle \mathcal{P}(^1S_0^{[8]}) \rangle_{h_c}}{m_c^4} = 0.561_{-0.197}^{+0.350} \text{ MeV}. \end{aligned} \quad (41)$$

The errors are estimated by varying m_c and μ_{Λ_0} , among which, the uncertainty of μ_{Λ_0} dominates the errors for the two S -wave LDMEs.

Using the same method we can determine the LDMEs for h_b ,

$$\begin{aligned} \langle \bar{\mathcal{O}}(^1P_1^{[1]}) \rangle_{h_b} &= 0.7555_{-0.0623}^{+0.0694} \text{ MeV}, \\ \langle \bar{\mathcal{P}}(^1P_1^{[1]}) \rangle_{h_b} &= 0.0314_{-0.0026}^{+0.0029} \text{ MeV}, \\ \langle \bar{\mathcal{O}}(^1S_0^{[8]}) \rangle_{h_b} &= 0.3959_{-0.0503}^{+0.0611} \text{ MeV}, \\ \langle \bar{\mathcal{P}}(^1S_0^{[8]}) \rangle_{h_b} &= 0.0169_{-0.0022}^{+0.0026} \text{ MeV}. \end{aligned} \quad (42)$$

Here we choose $m_b = 4.6 \pm 0.1$ GeV, $\mu_{\Lambda_0} = m_b v \sim 1.5 \pm 0.2$ GeV, and set $\langle \mathbf{v}^2 \rangle_{h_b} \approx \langle \mathbf{v}^2 \rangle_{\eta_b}$, similar to the assumption for h_c .

Note that another method to determine the value of the color-octet LDME $\langle \mathcal{O}(^1S_0^{[8]}) \rangle_{h_c}$ at leading order in v is provided in Ref. [36], where LDMEs are further factorized by potential-NRQCD factorization, and they are then expressed in terms of gluonic vacuum condensation factor $\mathcal{E}(\mu)$. In Ref. [36] they gave both its evolution equation and

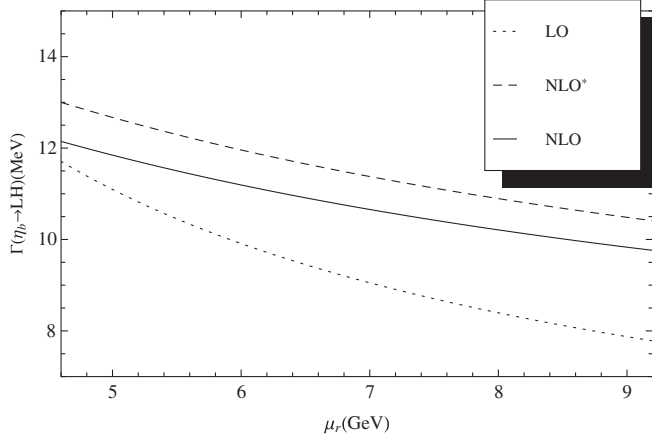


FIG. 5. μ_r dependence of $\Gamma(\eta_b \rightarrow \text{LH})$. LO represents values without QCD and relativistic corrections, NLO* includes QCD corrections but only at leading order in v , and NLO takes into account all contributions up to $O(\alpha_s v^2)$. The LDMEs are taken from the B-T potential model and the Gremm-Kapustin relation. Here we set $\mu_\Lambda = 2m_b$, and $m_b = 4.6$ GeV.

the initial value at the scale $\mu_0 = 1$ GeV. We evolve this factor from the initial scale to $2m_c$ and find that the value of $\langle \bar{\mathcal{O}}(^1S_0^{[8]}) \rangle_{h_c}$ through this method is about 3.5 MeV, which is a little larger than our result. However, the derivation is reasonable since we include the relativistic corrections which essentially decrease the value at leading order in v [see the second term at the right-hand of the first line in Eq. (40)].

B. $\Gamma(\eta_b \rightarrow \text{LH})$

We now discuss the hadronic decay width of η_b based on the values of LDMEs given above. Let's first fix both the renormalization scale μ_r and factorization scale μ_Λ to be $2m_b$ and consider the uncertainty introduced by LDMEs. For this choice of scales, the decay width can be written as

$$\Gamma(\eta_b \rightarrow \text{LH}) = 427.4_{-5.7}^{+5.9} \times 10^{-3} \langle \bar{\mathcal{O}}(^1S_0^{[1]}) \rangle_{\eta_b} - 641.4_{-9.2}^{+8.8} \times 10^{-3} \langle \bar{\mathcal{P}}(^1S_0^{[1]}) \rangle_{\eta_b}, \quad (43)$$

where errors are estimated by varying $m_b = 4.6 \pm 0.1$ GeV, and LDMEs $\langle \bar{\mathcal{O}}(^1S_0^{[1]}) \rangle_{\eta_b}$ and $\langle \bar{\mathcal{P}}(^1S_0^{[1]}) \rangle_{\eta_b}$ are given by Eq. (37). As the coefficients for $\langle \bar{\mathcal{O}}(^1S_0^{[1]}) \rangle_{\eta_b}$ and $\langle \bar{\mathcal{P}}(^1S_0^{[1]}) \rangle_{\eta_b}$ are at the same order, the smallness of $\langle \bar{\mathcal{P}}(^1S_0^{[1]}) \rangle_{\eta_b}$ means the relativistic correction can only change the total decay width by about 5%, which is not important as expected. Considering also the correlation between errors, we get the hadronic decay width of η_b with the choice of $\mu_r = \mu_\Lambda = 2m_b$,

$$\Gamma(\eta_b \rightarrow \text{LH}) = 9.76_{-0.54}^{+0.58} \text{ MeV}. \quad (44)$$

We find the μ_Λ dependence is much weaker than the μ_r dependence, thus we only discuss the μ_r dependence here. By varying the μ_r , we get the μ_r dependence of hadronic decay width in Fig. 5. It is clear that the NLO calculation significantly reduces the μ_r dependence. Varying μ_r from m_b to $2m_b$, we get the decay width $\Gamma(\eta_b \rightarrow \text{LH}) \approx \Gamma^{\text{total}}(\eta_b) \sim 9.5\text{--}12$ MeV. This value is consistent with the experimental data $\Gamma^{\text{exp}}(\eta_b) = 10.8_{-3.7-2.0}^{+4.0+4.5}$ MeV [8].

C. $\Gamma(h_c \rightarrow \text{LH})$

The numerical values of the SD coefficients for hadronic decay width of h_c are

$$\begin{aligned} \Gamma(h_c \rightarrow \text{LH}) = & 328.7_{-21.8}^{+26.1} \times 10^{-3} \langle \bar{\mathcal{O}}(^1S_0^{[8]}) \rangle_{h_c} \\ & - 39.6_{-3.8}^{+3.1} \times 10^{-3} \langle \bar{\mathcal{O}}(^1P_1^{[1]}) \rangle_{h_c} \\ & - 446.0_{-35.5}^{+29.7} \times 10^{-3} \langle \bar{\mathcal{P}}(^1S_0^{[8]}) \rangle_{h_c} \\ & + 92.4_{-7.3}^{+8.8} \times 10^{-3} \langle \bar{\mathcal{P}}(^1P_1^{[1]}) \rangle_{h_c}, \end{aligned} \quad (45)$$

where both the renormalization scale μ_r and factorization scale μ_Λ are set to be $2m_c$. The redefined LDMEs and their values are given in Eq. (41). With these results we then investigate the effects of the QCD corrections and relativistic corrections.

Let us first analyze the partial widths of the four channels in Table I. Among the four, the $\langle \mathcal{O}(^1S_0^{[8]}) \rangle_{h_c}$ channel is positive and it dominates the total width. Contributions of the $\langle \mathcal{O}(^1P_1^{[1]}) \rangle_{h_c}$ channel and $\langle \mathcal{P}(^1S_0^{[8]}) \rangle_{h_c}$ channel are negative and compatible, although the latter one is suppressed by v^2 . This is because, as we mentioned before, the $^1P_1^{[1]}$ Fock state cannot couple with two gluons, and its SD coefficient is suppressed by α_s . It is the balance between α_s and v^2 that results in the two partial decay widths being compatible. The last term, $\langle \mathcal{P}(^1P_1^{[1]}) \rangle_{h_c}$ channel, is suppressed by both α_s and v^2 , and it gives the smallest contribution. Summing up the first two channels we get the decay width at leading order in v , $\Gamma(v^0) = 0.53_{-0.23}^{+0.40}$ MeV, which is consistent with the previous work [17]. However, we will show later that the experimental data favor a smaller value. Including also the relativistic corrections, the total decay width will decrease by about 1/3. Next we list the partial widths order by order in α_s and v in Table II. We find the QCD correction, $\alpha_s^1 v^0$ contribution, is as large as the leading order contribution. Detailed study reveals that the large correction mainly comes from the $^1S_0^{[8]}$ channel. In Ref. [37], the authors

TABLE I. $\Gamma(h_c \rightarrow \text{LH})$ expressed with the contributions of each LDME.

	$\langle \mathcal{O}(^1S_0^{[8]}) \rangle_{h_c}$	$\langle \mathcal{O}(^1P_1^{[1]}) \rangle_{h_c}$	$\langle \mathcal{P}(^1S_0^{[8]}) \rangle_{h_c}$	$\langle \mathcal{P}(^1P_1^{[1]}) \rangle_{h_c}$	Total
$\Gamma(^2S+1L_J^c \rightarrow \text{LH})$ (MeV)	$0.67_{-0.25}^{+0.43}$	$-0.14_{-0.06}^{+0.04}$	$-0.25_{-0.17}^{+0.10}$	$0.07_{-0.02}^{+0.03}$	$0.35_{-0.15}^{+0.25}$

TABLE II. $\Gamma(h_c \rightarrow \text{LH})$ expressed with contributions at various orders of α_s and \mathbf{v} .

	$\alpha_s^0 v^0$	$\alpha_s^1 v^0$	$\alpha_s^0 v^2$	$\alpha_s^1 v^2$	Total
$\Gamma(h_c \rightarrow \text{LH})$ (MeV)	$0.32^{+0.21}_{-0.12}$	$0.21^{+0.20}_{-0.11}$	$-0.12^{+0.04}_{-0.08}$	$-0.06^{+0.04}_{-0.08}$	$0.35^{+0.25}_{-0.15}$

pointed out that the large correction for the $^1S_0^{[1]}$ channel, similar to the $^1S_0^{[8]}$ channel, is due to the existence of renormalons, and they also proposed a resummation method to deal with the renormalons. Nevertheless, resummation of this kind for the $^1S_0^{[8]}$ channel is beyond the scope of this work, and we will leave it as a future study. In our work, as both the $\alpha_s^0 v^2$ contribution and the $\alpha_s^1 v^2$ contribution are negative, they can balance the enhancement by QCD correction of the $^1S_0^{[8]}$ channel. Moreover, we find our complete NLO correction improves the normalization and factorization scale dependence compared with the NLO* results, which are shown in Fig. 6.

In order to compare with the experiment data [5], we also need the E1 transition decay width $\Gamma(h_c \rightarrow \eta_c + \gamma)$ up to the v^2 order, because this is another important decay channel of h_c . Reference [17] estimated the transition decay widths but only at leading order in v by using HQSS between the spin-singlet and triplet P -wave charmonia,

$$\Gamma(h_c \rightarrow \gamma \eta_c) = \frac{(E_\gamma^{h_c})^3}{9} \sum_{J=0}^2 (2J+1) \frac{\Gamma(\chi_{cJ} \rightarrow \gamma J/\psi)}{(E_\gamma^{\chi_{cJ}})^3}. \quad (46)$$

And the obtained E1 width is 615 ± 29 keV using the PDG data [30]. This result is consistent with the potential model

calculations at leading order in v [38]. However, if the v^2 corrections are considered, HQSS will not hold any more. Reference [38] showed that the width of $h_c \rightarrow \gamma \eta_c$ can be reduced from 650 to 385 keV by relativistic effects. Subsequent studies using various potential models [39–41] also observed similar relativistic effects, resulting in E1 transition width at the range of 354–323 keV. In this paper we choose the value $\Gamma(h_c \rightarrow \gamma \eta_c) = 385$ keV from Ref. [38].

Combining the LH and $\gamma \eta_c$ decay channels of h_c , we get the predictions for total decay width $\Gamma^{\text{th}}(h_c) = 0.74^{+0.25}_{-0.15}$ MeV and the branching ratio $\mathcal{B}^{\text{th}}(h_c \rightarrow \eta_c + \gamma) = 52 \pm 13\%$. Our predictions are consistent with the new experimental data $\Gamma^{\text{exp}}(h_c) = 0.73^{+0.45}_{-0.28}$ MeV and $\mathcal{B}^{\text{exp}}(h_c \rightarrow \eta_c + \gamma) = 54.3 \pm 6.7 \pm 5.2\%$ measured by the BESIII Collaboration [5]. However, if we ignore the relativistic corrections to the hadronic decay width, the total width will increase to 0.92 MeV and the E1 transition branching ratio will be decreased to 42%. Therefore, it is evident that the relativistic corrections play an important role in the h_c decay and they can lead to a better agreement between theoretical prediction and the experimental data.

D. $\Gamma(h_b \rightarrow \text{LH})$

Similar to h_c , we get the decay width for h_b ,

$$\begin{aligned} \Gamma(h_b \rightarrow \text{LH}) = & 145.9^{+2.1}_{-2.0} \times 10^{-3} \langle \bar{\mathcal{O}}(^1S_0^{[8]}) \rangle_{h_b} \\ & - (15.3 \pm 0.3) \times 10^{-3} \langle \bar{\mathcal{O}}(^1P_1^{[1]}) \rangle_{h_b} \\ & - (196.0 \pm 3.0) \times 10^{-3} \langle \bar{\mathcal{P}}(^1S_0^{[8]}) \rangle_{h_b} \\ & + (35.8 \pm 0.6) \times 10^{-3} \langle \bar{\mathcal{P}}(^1P_1^{[1]}) \rangle_{h_b}. \end{aligned} \quad (47)$$

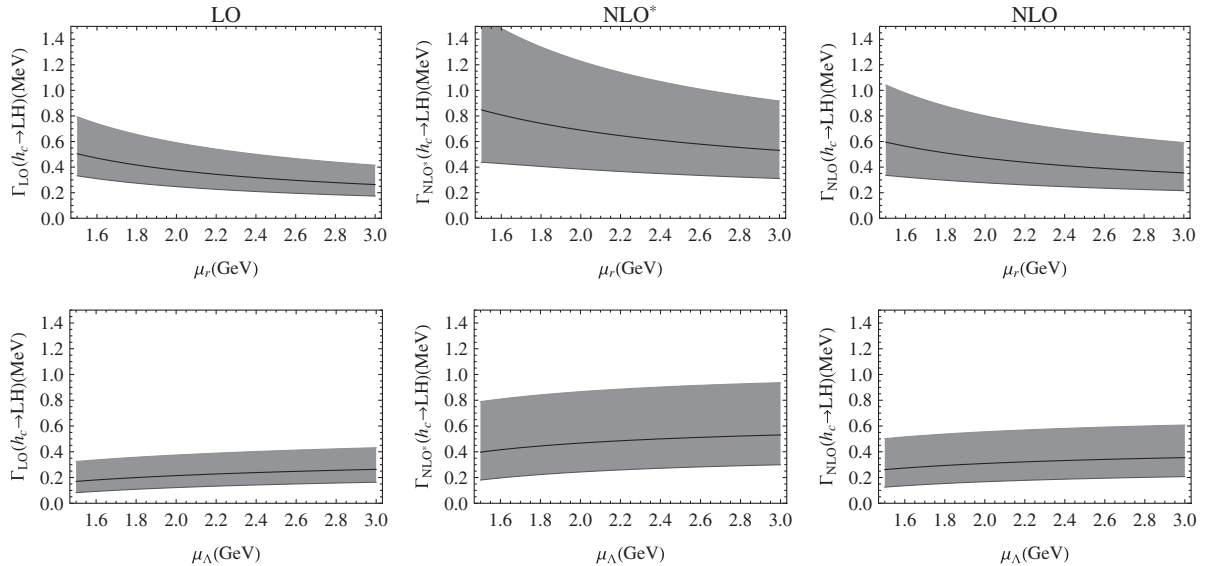


FIG. 6. μ_r and μ_Λ dependence of $\Gamma(h_c \rightarrow \text{LH})$. The upper plots are for μ_r and lower ones for μ_Λ . From left to right the plots are shown for LO, NLO*, and NLO, respectively, where NLO* includes $O(\alpha_s)$ but excludes $O(\alpha_s v^2)$ corrections.

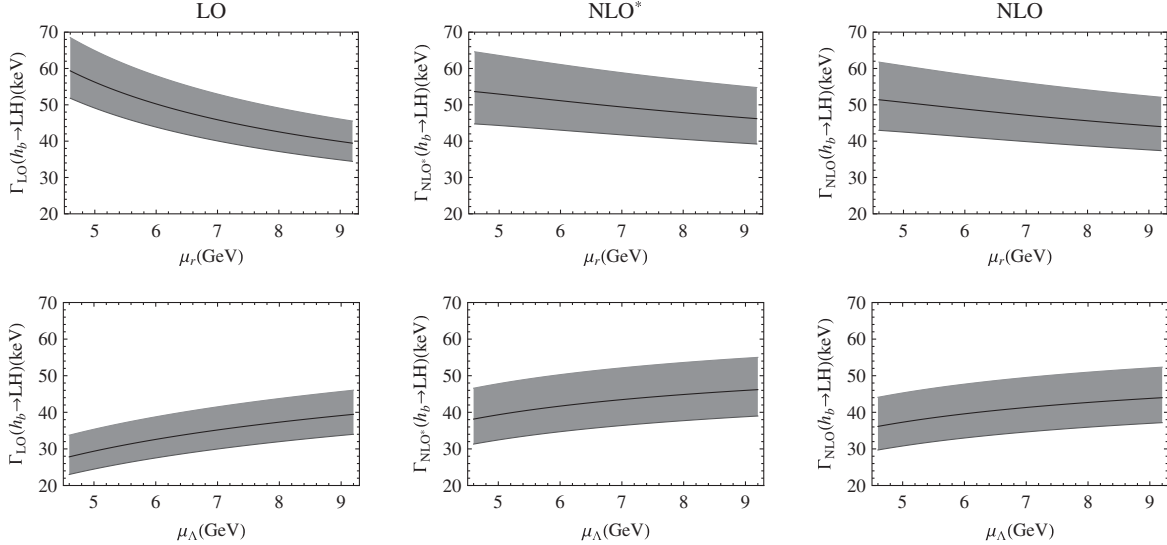


FIG. 7. μ_r and μ_Λ dependence of $\Gamma(h_b \rightarrow \text{LH})$. From left to right the three plots represent LO, NLO*, and NLO, respectively, where NLO* includes $O(\alpha_s)$ but excludes $O(\alpha_s v^2)$ corrections.

The μ_r and μ_Λ dependence are plotted in Fig. 7, where again we find the complete NLO correction largely reduces the scale dependence. From the partial decay width of each contribution in Tables III and IV, it is clear that the v^2 correction effect is much smaller for h_b than that for h_c , while QCD correction is still important. The E1 transition decay width for h_b is evaluated in the NR [42], GI [41], and screened-potential models [43], and the results are listed in Table V. Compared with the experiment data $\mathcal{B}^{\text{exp}}(h_b(1P) \rightarrow \eta_b(1S)\gamma) = 49.2 \pm 5.7^{+5.6}_{-3.3}\%$ [8], our

prediction using the NR model fits it very well, and predictions using the other three models are also within the error band.

VI. SUMMARY

We have calculated order $\alpha_s v^2$ corrections for the annihilation hadronic decay widths of spin-singlet heavy quarkonia η_b , h_c , and h_b within the framework of NRQCD. The short-distance coefficients are calculated by covariant projection method, and the LDMEs are estimated by using

TABLE III. $\Gamma(h_b \rightarrow \text{LH})$ expressed with contributions of each LDME.

	$\langle \mathcal{O}(^1S_0^{[8]}) \rangle_{h_b}$	$\langle \mathcal{O}(^1P_1^{[1]}) \rangle_{h_b}$	$\langle \mathcal{P}(^1S_0^{[8]}) \rangle_{h_b}$	$\langle \mathcal{P}(^1P_1^{[1]}) \rangle_{h_b}$	Total
$\Gamma(^{2S+1}L_J^{[c]} \rightarrow \text{LH})$ (keV)	$57.78^{+9.42}_{-7.79}$	$-11.58^{+1.13}_{-1.29}$	$-3.32^{+0.45}_{-0.54}$	$1.12^{+0.12}_{-0.11}$	$44.00^{+8.23}_{-6.73}$

TABLE IV. $\Gamma(h_b \rightarrow \text{LH})$ expressed with various orders of α_s and v .

	$\alpha_s^0 v^0$	$\alpha_s^1 v^0$	$\alpha_s^0 v^2$	$\alpha_s^1 v^2$	Total
$\Gamma(h_b \rightarrow \text{LH})$ (keV)	$33.41^{+5.39}_{-4.46}$	$12.78^{+3.39}_{-2.72}$	$-1.91^{+0.26}_{-0.31}$	$-0.29^{+0.15}_{-0.19}$	$44.00^{+8.23}_{-6.73}$

TABLE V. $\Gamma(h_b \rightarrow \eta_b + \gamma)$ and $\mathcal{B}(h_b \rightarrow \eta_b + \gamma)$ in NR, GI, and screened-potential models (SNR₀ is calculated using the zeroth-order wave functions and SNR₁, using the first-order relativistically corrected wave functions).

	NR	GI	SNR ₀	SNR ₁
$\Gamma(h_b \rightarrow \eta_b + \gamma)$ (keV)	41.8	37.0	55.8	36.3
$\Gamma_{\text{total}}(h_b)$ (keV)	85.8	81.0	100.0	80.3
$\mathcal{B}(h_b \rightarrow \eta_b + \gamma)$	48.7%	45.7%	55.9%	45.2%

the potential model and operator evolution methods. For the h_c decay, we find that $O(v^2)$ and $O(\alpha_s v^2)$ corrections contribute large and negative values to the decay width, which substantially reduce the decay width calculated in the leading order in v^2 . It shows that relativistic corrections play an important role in hadronic decays of the $c\bar{c}$ system, and can improve the theoretical results as compared with experimental data. Our calculated total decay width $\Gamma^{\text{th}}(h_c) = 0.74^{+0.25}_{-0.15}$ MeV and branching ratio $\mathcal{B}^{\text{th}}(h_c \rightarrow \eta_c + \gamma) = 52 \pm 13\%$ are consistent with the measurements by BESIII [5]. For η_b and h_b decays, we have calculated their hadronic decay widths and found that $\Gamma(\eta_b \rightarrow \text{LH}) = 9.76^{+0.58}_{-0.54}$ MeV and $\Gamma(h_b \rightarrow \text{LH}) = 44.00^{+8.23}_{-6.73}$ keV. We conclude that for the $b\bar{b}$ system $O(\alpha_s v^2)$ corrections are not as important as in the $c\bar{c}$ system. We have also compared our theoretical results with experimental data [5,8] and found that in general our calculations are consistent with data within theoretical and experimental uncertainties.

ACKNOWLEDGMENTS

We are grateful to B. Q. Li, C. Meng, J. W. Qiu, and M. Stratmann for many helpful discussions. This work was supported in part by the National Natural Science Foundation of China (No. 11021092 and No. 11075002),

and the Ministry of Science and Technology of China (No. 2009CB825200). Y.Q.M is supported by the U.S. Department of Energy, Contract No. DE-AC02-98CH10886.

APPENDIX A: EVOLUTION OF NRQCD MATRIX ELEMENTS $\mathcal{O}(^1S_0^{[8]})$ AND $\mathcal{P}(^1S_0^{[8]})$ AT $O(\alpha_s v^2)$

In order to cancel the infrared divergence in short-distance coefficients of the $^1P_1^{[1]}$ Fock state, we need to evaluate the NRQCD four-fermion operators $\mathcal{O}(^1S_0^{[8]})$ and $\mathcal{P}(^1S_0^{[8]})$ to sufficient order.

The $O(\alpha_s)$ correction diagrams include the following three sets: self-energy diagrams which are related to self-energy corrections of external heavy (anti-)quarks; Coulomb diagrams, where the gluon is connected with both initial or final heavy quark and antiquark; and the intersecting diagrams, where the gluon is related to an initial heavy (anti-)quark and a final (anti-)quark. The results of the first two sets have been given in Refs. [20,44], and here we only calculate the intersecting diagrams that relate to the transition from S wave to P wave.

Using the Lagrangian shown in Eqs. (3) and (5), we can write the amplitudes of diagrams in Fig. 8 as (other crossed diagrams are not shown)

$$I_{a+b+c} = ig_s^2 \int \frac{d^D l}{(2\pi)^D} \frac{\mathbf{q} \cdot \mathbf{q}' - (\mathbf{q} \cdot \mathbf{l})(\mathbf{q}' \cdot \mathbf{l})/l^2}{m_Q^2(l_0^2 - l^2 + i\epsilon)} \frac{1 - \mathbf{q}^2/2m_Q^2 - \mathbf{q}'^2/2m_Q^2}{[q_0 - l_0 - \frac{(\mathbf{q}-\mathbf{l})^2}{2m_Q} + i\epsilon][q'_0 - l_0 - \frac{(\mathbf{q}'-\mathbf{l})^2}{2m_Q} + i\epsilon]}, \quad (\text{A1a})$$

$$I_d = ig_s^2 \int \frac{d^D l}{(2\pi)^D} \frac{-1}{[q_0 - l_0 - \frac{(\mathbf{q}-\mathbf{l})^2}{2m_Q} + i\epsilon][q'_0 - l_0 - \frac{(\mathbf{q}'-\mathbf{l})^2}{2m_Q} + i\epsilon]}, \quad (\text{A1b})$$

where $q = (q_0, \mathbf{q})$ is the heavy quark external momentum and $l = (l_0, \mathbf{l})$ is the loop integral momentum. Since there is no pole on the upper half of the l_0 's complex plane, the second integral I_d yields zero. Contour integrating the first integral over l_0 around the $l_0 = |\mathbf{l}| - i\epsilon$ pole, we find

$$I_{a+b+c} = g_s^2 \int \frac{d^{D-1} l}{(2\pi)^{D-1}} \frac{\mathbf{q} \cdot \mathbf{q}' - (\mathbf{q} \cdot \mathbf{l})(\mathbf{q}' \cdot \mathbf{l})/l^2}{2m_Q^2|\mathbf{l}|} \frac{1 - \mathbf{q}^2/2m_Q^2 - \mathbf{q}'^2/2m_Q^2}{[-|\mathbf{l}| - \frac{l^2}{2m_Q} + \frac{\mathbf{q} \cdot \mathbf{l}}{m_Q} + i\epsilon][-|\mathbf{l}| - \frac{l^2}{2m_Q} + \frac{\mathbf{q}' \cdot \mathbf{l}}{m_Q} + i\epsilon]}. \quad (\text{A2})$$

Before further performing the integration, we will expand the relative momentum in the denominator [45]. Assuming that $\mathbf{q} \cdot \mathbf{l}/m_Q$, $\mathbf{q}' \cdot \mathbf{l}/m_Q$, and l^2/m_Q are far smaller than $|\mathbf{l}|$, we get the required expansion,

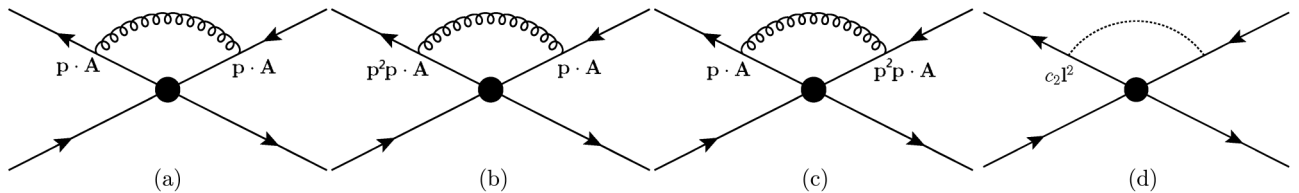


FIG. 8. The one-loop NRQCD diagrams which involve the Feynman rules up to $O(v^2)$. The Coulomb interactions and the cross diagrams have been suppressed.

$$I_{a+b+c} = \frac{g_s^2}{2m_Q^2} \int \frac{d^{D-1}l}{(2\pi)^{D-1}} \frac{\mathbf{q} \cdot \mathbf{q}' - (\mathbf{q} \cdot \mathbf{l})(\mathbf{q}' \cdot \mathbf{l})/l^2}{|\mathbf{l}|^3} (1 - \mathbf{q}^2/2m_Q^2 - \mathbf{q}'^2/2m_Q^2) \left(1 + \left(\frac{\mathbf{q} \cdot \mathbf{l}}{|\mathbf{l}|m_Q} \right)^2 + \left(\frac{\mathbf{q}' \cdot \mathbf{l}}{|\mathbf{l}|m_Q} \right)^2 \right) + (\text{high order or irrelevant expansions}). \quad (\text{A3})$$

This integral can be reduced by taking the following substitution,

$$l^i l^j \rightarrow \frac{1}{D-1} \delta^{ij} l^2, \quad (\text{A4a})$$

$$l^i l^j l^k l^r \rightarrow \frac{1}{(D-1)(D+1)} (\delta^{ij} \delta^{kr} + \delta^{ik} \delta^{jr} + \delta^{ir} \delta^{kj}) l^4, \quad (\text{A4b})$$

where δ^{ij} is the $D-1$ dimensional Euclidean delta symbol. The integral yields

$$I_{a+b+c} = \frac{\pi \alpha_s^{(b)}}{2m_Q^2} \frac{\mathbf{q} \cdot \mathbf{q}'}{\pi^2} \frac{D-2}{D-1} \left(1 - \frac{D-1}{D+1} \frac{1}{2m_Q^2} (\mathbf{q}^2 + \mathbf{q}'^2) \right) \left(\frac{1}{\epsilon_{\text{UV}}} - \frac{1}{\epsilon_{\text{IR}}} \right). \quad (\text{A5})$$

Summing up all the diagrams we get

$$I = \frac{2\alpha_s^{(b)}}{\pi m_Q^2} \frac{D-2}{D-1} \mathbf{q} \cdot \mathbf{q}' \left(\frac{1}{\epsilon_{\text{UV}}} - \frac{1}{\epsilon_{\text{IR}}} \right) \left(1 - \frac{D-1}{D+1} \frac{1}{2m_Q^2} (\mathbf{q}^2 + \mathbf{q}'^2) \right) \left[C_F \frac{1 \otimes 1}{2N_c} + B_F T^a \otimes T^a \right] \mathcal{O}(^1 S_0^{[8]}). \quad (\text{A6})$$

Recalling the definitions of $\mathcal{O}(^1 P_1^{[1]})$ and $\mathcal{P}(^1 P_1^{[1]})$, we can write

$$\langle H | \mathcal{O}(^1 S_0^{[8]}) | H \rangle = \langle H | \mathcal{O}(^1 S_0^{[8]}) | H \rangle_{\text{Bom}} + \frac{2(D-2)\alpha_s^{(b)}}{(D-1)\pi m_Q^2} \left(\frac{1}{\epsilon_{\text{UV}}} - \frac{1}{\epsilon_{\text{IR}}} \right) \left[C_F \frac{\langle H | \mathcal{O}(^1 P_1^{[1]}) | H \rangle}{2N_c} - \frac{D-1}{(D+1)m_Q^2} C_F \frac{\langle H | \mathcal{P}(^1 P_1^{[1]}) | H \rangle}{2N_c} \right], \quad (\text{A7a})$$

$$\langle H | \mathcal{P}(^1 S_0^{[8]}) | H \rangle = \langle H | \mathcal{P}(^1 S_0^{[8]}) | H \rangle_{\text{Bom}} + \frac{2(D-2)\alpha_s^{(b)}}{(D-1)\pi m_Q^2} \left(\frac{1}{\epsilon_{\text{UV}}} - \frac{1}{\epsilon_{\text{IR}}} \right) C_F \frac{\langle H | \mathcal{P}(^1 P_1^{[1]}) | H \rangle}{2N_c}, \quad (\text{A7b})$$

where we have omitted terms for $\mathcal{O}(^1 P_1^{[8]})$ and $\mathcal{P}(^1 P_1^{[8]})$, since they are irrelevant in our work. The presence of UV divergence indicates that the LDMEs need renormalization. The relevant counterterm in the $\overline{\text{MS}}$ scheme can be chosen as

$$\langle H | \mathcal{O}(^1 S_0^{[8]}) | H \rangle = \mu_\Lambda^{-2\epsilon} \left\{ \langle H | \mathcal{O}(^1 S_0^{[8]}) | H \rangle^{(\mu_\Lambda)} + \frac{4\alpha_s}{3\pi m_Q^2} \left(\frac{1}{\epsilon_{\text{UV}}} + \ln 4\pi - \gamma_E \right) \left[C_F \frac{\langle H | \mathcal{O}(^1 P_1^{[1]}) | H \rangle}{2N_c} - \frac{3}{5m_Q^2} C_F \frac{\langle H | \mathcal{P}(^1 P_1^{[1]}) | H \rangle}{2N_c} \right] \right\}, \quad (\text{A8a})$$

$$\langle H | \mathcal{P}(^1 S_0^{[8]}) | H \rangle = \mu_\Lambda^{-2\epsilon} \left\{ \langle H | \mathcal{P}(^1 S_0^{[8]}) | H \rangle^{(\mu_\Lambda)} + \frac{4\alpha_s}{3\pi m_Q^2} \left(\frac{1}{\epsilon_{\text{UV}}} + \ln 4\pi - \gamma_E \right) C_F \frac{\langle H | \mathcal{P}(^1 P_1^{[1]}) | H \rangle}{2N_c} \right\}, \quad (\text{A8b})$$

where μ_Λ is the NRQCD renormalization scale. Combining Eqs. (A7) and (A8), we find

$$\begin{aligned} \langle H | \mathcal{O}(^1 S_0^{[8]}) | H \rangle_{\text{Bom}} &= \mu_\Lambda^{-2\epsilon} \langle H | \mathcal{O}(^1 S_0^{[8]}) | H \rangle^{(\mu_\Lambda)} + \frac{4\alpha_s}{3\pi m_Q^2} \left(\frac{1}{\epsilon_{\text{IR}}} + \ln 4\pi - \gamma_E \right) \left(\frac{\mu}{\mu_\Lambda} \right)^{2\epsilon} \\ &\quad \times \left[C_F \frac{\langle H | \mathcal{O}(^1 P_1^{[1]}) | H \rangle}{2N_c} - \frac{3}{5m_Q^2} C_F \frac{\langle H | \mathcal{P}(^1 P_1^{[1]}) | H \rangle}{2N_c} \right], \end{aligned} \quad (\text{A9a})$$

$$\langle H | \mathcal{P}(^1 S_0^{[8]}) | H \rangle_{\text{Bom}} = \mu_\Lambda^{-2\epsilon} \langle H | \mathcal{P}(^1 S_0^{[8]}) | H \rangle^{(\mu_\Lambda)} + \frac{4\alpha_s}{3\pi m_Q^2} \left(\frac{1}{\epsilon_{\text{IR}}} + \ln 4\pi - \gamma_E \right) \left(\frac{\mu}{\mu_\Lambda} \right)^{2\epsilon} C_F \frac{\langle H | \mathcal{P}(^1 P_1^{[1]}) | H \rangle}{2N_c}. \quad (\text{A9b})$$

Considering also the self-energy contribution [see Eq. (B14) in Ref. [1]], we get the total loop corrections of NRQCD LDMEs,

$$\begin{aligned} \langle H|\mathcal{O}(^1S_0^{[8]}|H)\rangle_{\text{Born}} &= \mu_\Lambda^{-2\epsilon} \langle H|\mathcal{O}(^1S_0^{[8]}|H)\rangle^{(\mu_\Lambda)} + \frac{4\alpha_s}{3\pi m_Q^2} \left(\frac{1}{\epsilon_{\text{IR}}} + \ln 4\pi - \gamma_E \right) \left(\frac{\mu}{\mu_\Lambda} \right)^{2\epsilon} \\ &\quad \times \left[C_F \frac{\langle H|\mathcal{O}(^1P_1^{[1]}|H)\rangle}{2N_c} - \frac{3}{5m_Q^2} C_F \frac{\langle H|\mathcal{P}(^1P_1^{[1]}|H)\rangle}{2N_c} - \frac{N_c^2 - 2}{4N_c} \langle H|\mathcal{P}(^1S_0^{[8]}|H)\rangle \right], \end{aligned} \quad (\text{A10a})$$

$$\langle H|\mathcal{P}(^1S_0^{[8]}|H)\rangle_{\text{Born}} = \mu_\Lambda^{-2\epsilon} \langle H|\mathcal{P}(^1S_0^{[8]}|H)\rangle^{(\mu_\Lambda)} + \frac{4\alpha_s}{3\pi m_Q^2} \left(\frac{1}{\epsilon_{\text{IR}}} + \ln 4\pi - \gamma_E \right) \left(\frac{\mu}{\mu_\Lambda} \right)^{2\epsilon} C_F \frac{\langle H|\mathcal{P}(^1P_1^{[1]}|H)\rangle}{2N_c}. \quad (\text{A10b})$$

APPENDIX B: SCHEME CHOICE AND ABSORPTION OF $\langle \mathcal{T}_{1-8}(^1S_0, ^1P_1) \rangle_{iP_1}$

In this appendix, we define the factorization scheme that we use in this work, and we will show that there is no contribution from $\langle \mathcal{T}_{1-8}(^1S_0, ^1P_1) \rangle_{iP_1}$ in our scheme. Let's begin with the factorization formula for $\Gamma(H(^1P_1) \rightarrow \text{LH})$ in the $\overline{\text{MS}}$ scheme,

$$\begin{aligned} \Gamma(H(^1P_1) \rightarrow \text{LH}) &= \frac{F(^1S_0^{[8]})_{\overline{\text{MS}}}}{m_Q^2} \langle \mathcal{O}(^1S_0^{[8]}) \rangle_{iP_1}^{\overline{\text{MS}}} + \frac{G(^1S_0^{[8]})_{\overline{\text{MS}}}}{m_Q^4} \langle \mathcal{P}(^1S_0^{[8]}) \rangle_{iP_1}^{\overline{\text{MS}}} + \frac{F(^1P_1^{[1]})_{\overline{\text{MS}}}}{m_Q^4} \langle \mathcal{O}(^1P_1^{[1]}) \rangle_{iP_1}^{\overline{\text{MS}}} \\ &\quad + \frac{G(^1P_1^{[1]})_{\overline{\text{MS}}}}{m_Q^6} \langle \mathcal{P}(^1P_1^{[1]}) \rangle_{iP_1}^{\overline{\text{MS}}} + \frac{T(^1S_0, ^1P_1)_{\overline{\text{MS}}}}{m_Q^5} \langle \mathcal{T}_{1-8}(^1S_0, ^1P_1) \rangle_{iP_1}^{\overline{\text{MS}}}, \end{aligned} \quad (\text{B1})$$

where an explicit $\overline{\text{MS}}$ is marked for any LDME and SD coefficient. There are many scheme choices to eliminate the last term in Eq. (B1). Our choice is to define the factorization scheme of $\langle \mathcal{O}(^1S_0^{[8]}) \rangle_{iP_1}$ by the following relation,

$$\begin{aligned} \Gamma(H(^1P_1) \rightarrow \text{LH}) &= \frac{F(^1S_0^{[8]})_{\overline{\text{MS}}}}{m_Q^2} \langle \mathcal{O}(^1S_0^{[8]}) \rangle_{iP_1}^{\text{LT}} + \frac{G(^1S_0^{[8]})_{\overline{\text{MS}}}}{m_Q^4} \langle \mathcal{P}(^1S_0^{[8]}) \rangle_{iP_1}^{\overline{\text{MS}}} + \frac{F(^1P_1^{[1]})_{\overline{\text{MS}}}}{m_Q^4} \langle \mathcal{O}(^1P_1^{[1]}) \rangle_{iP_1}^{\overline{\text{MS}}} \\ &\quad + \frac{G(^1P_1^{[1]})_{\overline{\text{MS}}}}{m_Q^6} \langle \mathcal{P}(^1P_1^{[1]}) \rangle_{iP_1}^{\overline{\text{MS}}}, \end{aligned} \quad (\text{B2})$$

where, to distinguish from the $\overline{\text{MS}}$ scheme, we denote it as the leading twist scheme (LT). Note that the relation in Eq. (B2) should be understood to be valid only at α_s order, that is, $T(^1S_0, ^1P_1)^{\text{LT}}$ can be nonzero at higher order in α_s . From Eqs. (B1) and (B2), we get the scheme transformation relation,

$$\langle \mathcal{O}(^1S_0^{[8]}) \rangle_{iP_1}^{\text{LT}} - \langle \mathcal{O}(^1S_0^{[8]}) \rangle_{iP_1}^{\overline{\text{MS}}} = \frac{T(^1S_0, ^1P_1)_{\overline{\text{MS}}}}{m_Q^3 F(^1S_0^{[8]})_{\overline{\text{MS}}}} \langle \mathcal{T}_{1-8}(^1S_0, ^1P_1) \rangle_{iP_1}^{\overline{\text{MS}}}. \quad (\text{B3})$$

According to the α_s expansion of SD coefficients,

$$F(^1S_0^{[8]})_{\overline{\text{MS}}} = F(^1S_0^{[8]})^{(0)} + \alpha_s F(^1S_0^{[8]})^{(1)\overline{\text{MS}}} + O(\alpha_s^2), \quad (\text{B4a})$$

$$T(^1S_0, ^1P_1)_{\overline{\text{MS}}} = \alpha_s T(^1S_0, ^1P_1)^{(1)\overline{\text{MS}}} + O(\alpha_s^2), \quad (\text{B4b})$$

we rewrite the difference as

$$\langle \mathcal{O}(^1S_0^{[8]}) \rangle_{iP_1}^{\text{LT}} - \langle \mathcal{O}(^1S_0^{[8]}) \rangle_{iP_1}^{\overline{\text{MS}}} = \alpha_s \frac{T(^1S_0, ^1P_1)^{(1)\overline{\text{MS}}}}{m_Q^3 F(^1S_0^{[8]})^{(0)}} \langle \mathcal{T}_{1-8}(^1S_0, ^1P_1) \rangle_{iP_1}^{\overline{\text{MS}}} + O(\alpha_s^2). \quad (\text{B5})$$

It is clear that the difference is suppressed by $O(\alpha_s v^2)$, Eq. (B2) does not determine the scheme choice of $\langle \mathcal{T}_{1-8}(^1S_0, ^1P_1) \rangle_{iP_1}$, and one can still choose $\overline{\text{MS}}$ or other schemes. The reason is that the scheme dependence of $\langle \mathcal{T}_{1-8}(^1S_0, ^1P_1) \rangle_{iP_1}$ is at higher order in α_s , which is irrelevant to our calculation. Note that the relation between our scheme and the $\overline{\text{MS}}$ scheme here is similar to the relation between the DIS scheme and $\overline{\text{MS}}$ scheme

definition for the F_2 structure function of virtual γ deep inelastic scattering (see Refs. [46,47], for example).

An important consequence of Eq. (B5) is that the evolution equations for $\langle \mathcal{O}(^1S_0^{[8]}) \rangle_{iP_1}$ in both the $\overline{\text{MS}}$ and LT scheme at $O(\alpha_s)$ are exactly the same, which follows from the fact that the factorization scale dependence of both $T(^1S_0, ^1P_1)^{(1)\overline{\text{MS}}}$ and $\langle \mathcal{T}_{1-8}(^1S_0, ^1P_1) \rangle_{iP_1}^{\overline{\text{MS}}}$ are at $O(\alpha_s)$.

Therefore, although we calculate evolution equations for LDMEs in the $\overline{\text{MS}}$ scheme in Appendix A, these results are unchanged for the LT scheme.

Especially, the estimated $\langle \mathcal{O}(^1S_0^{[8]}) \rangle_{1P_1}$ in Sec. VA using OEM is the same for both the LT scheme and $\overline{\text{MS}}$ scheme. This seems to be questionable at first glance, as Eq. (B5) may imply its value is different under the two different

schemes. However, remember that the OEM picks up only the evolution terms in the LDMEs and disregards all other terms. Although Eq. (B5) tells us that $\langle \mathcal{O}(^1S_0^{[8]}) \rangle_{1P_1}$ is different under the two schemes, the difference only changes the initial value, which is ignored in the OEM. As a result, in the OEM this difference is ignored.

-
- [1] G. T. Bodwin, E. Braaten and G. P. Lepage, *Phys. Rev. D* **51**, 1125 (1995); **55**, 5853(E) (1997).
- [2] P. Rubin *et al.* (CLEO Collaboration), *Phys. Rev. D* **72**, 092004 (2005).
- [3] M. Andreotti, S. Bagnasco, W. Baldini, D. Bettoni, G. Borreani, A. Buzzo, R. Calabrese and R. Cester *et al.*, *Phys. Rev. D* **72**, 032001 (2005).
- [4] S. Dobbs *et al.* (CLEO Collaboration), *Phys. Rev. Lett.* **101**, 182003 (2008).
- [5] M. Ablikim *et al.* (BESIII Collaboration), *Phys. Rev. Lett.* **104**, 132002 (2010).
- [6] T. K. Pedlar *et al.* (CLEO Collaboration), *Phys. Rev. Lett.* **107**, 041803 (2011).
- [7] B. Aubert *et al.* (BABAR Collaboration), *Phys. Rev. Lett.* **101**, 071801 (2008); **102**, 029901(E) (2009).
- [8] R. Mizuk *et al.* (Belle Collaboration), *Phys. Rev. Lett.* **109**, 232002 (2012).
- [9] B. Aubert *et al.* (BABAR Collaboration), *Phys. Rev. Lett.* **103**, 161801 (2009).
- [10] G. Bonvicini *et al.* (CLEO Collaboration), *Phys. Rev. D* **81**, 031104 (2010).
- [11] I. Adachi *et al.* (Belle Collaboration), *Phys. Rev. Lett.* **108**, 032001 (2012).
- [12] J. Y. Ge *et al.* (CLEO Collaboration), *Phys. Rev. D* **84**, 032008 (2011).
- [13] H. W. Huang and K. T. Chao, *Phys. Rev. D* **54**, 3065 (1996); **56**, 7472(E) (1997); **60**, 079901(E) (1999).
- [14] A. Petrelli, *Phys. Lett. B* **380**, 159 (1996).
- [15] H. W. Huang and K. T. Chao, *Phys. Rev. D* **54**, 6850 (1996); **56**, 1821(E) (1997).
- [16] A. Petrelli, M. Cacciari, M. Greco, F. Maltoni, and M. L. Mangano, *Nucl. Phys.* **B514**, 245 (1998).
- [17] F. Maltoni, [arXiv:hep-ph/0007003](https://arxiv.org/abs/hep-ph/0007003).
- [18] Z.-G. He, Y. Fan and K.-T. Chao, *Phys. Rev. D* **81**, 074032 (2010).
- [19] Y. Fan, Z.-G. He, Y.-Q. Ma and K.-T. Chao, *Phys. Rev. D* **80**, 014001 (2009).
- [20] H.-K. Guo, Y.-Q. Ma and K.-T. Chao, *Phys. Rev. D* **83**, 114038 (2011).
- [21] N. Brambilla, A. Pineda, J. Soto, and A. Vairo, *Nucl. Phys.* **B566**, 275 (2000).
- [22] S. Fleming, I. Z. Rothstein, and A. K. Leibovich, *Phys. Rev. D* **64**, 036002 (2001).
- [23] A. Pineda and A. Vairo, *Phys. Rev. D* **63**, 054007 (2001); **64**, 039902(E) (2001).
- [24] N. Brambilla, E. Mereghetti, and A. Vairo, *Phys. Rev. D* **79**, 074002 (2009); **83**, 079904(E) (2011).
- [25] G. T. Bodwin and A. Petrelli, *Phys. Rev. D* **66**, 094011 (2002).
- [26] W.-Y. Keung and I. J. Muzinich, *Phys. Rev. D* **27**, 1518 (1983).
- [27] R. Mertig, M. Bohm, and A. Denner, *Comput. Phys. Commun.* **64**, 345 (1991).
- [28] T. Hahn, *Comput. Phys. Commun.* **140**, 418 (2001).
- [29] E. Eichten, K. Gottfried, T. Kinoshita, K. D. Lane and T.-M. Yan, *Phys. Rev. D* **17**, 3090 (1978); **21**, 313(E) (1980).
- [30] J. Beringer *et al.* (Particle Data Group Collaboration), *Phys. Rev. D* **86**, 010001 (2012).
- [31] W. Buchmuller and S. H. H. Tye, *Phys. Rev. D* **24**, 132 (1981).
- [32] E. J. Eichten and C. Quigg, *Phys. Rev. D* **52**, 1726 (1995).
- [33] D. Kang, T. Kim, J. Lee, and C. Yu, *Phys. Rev. D* **76**, 114018 (2007).
- [34] M. Gremm and A. Kapustin, *Phys. Lett. B* **407**, 323 (1997).
- [35] Y. Fan, J.-Z. Li, C. Meng and K.-T. Chao, *Phys. Rev. D* **85**, 034032 (2012).
- [36] N. Brambilla, D. Eiras, A. Pineda, J. Soto, and A. Vairo, *Phys. Rev. Lett.* **88**, 012003 (2001); N. Brambilla *et al.* (Quarkonium Working Group), [arXiv:hep-ph/0109130](https://arxiv.org/abs/hep-ph/0109130).
- [37] G. T. Bodwin and Y.-Q. Chen, *Phys. Rev. D* **64**, 114008 (2001).
- [38] K.-T. Chao, Y.-B. Ding and D.-H. Qin, *Phys. Lett. B* **301**, 282 (1993).
- [39] B.-Q. Li and K.-T. Chao, *Phys. Rev. D* **79**, 094004 (2009).
- [40] S. N. Gupta, J. M. Johnson, W. W. Repko, and C. J. Suchyta, III, *Phys. Rev. D* **49**, 1551 (1994).
- [41] S. Godfrey and J. L. Rosner, *Phys. Rev. D* **66**, 014012 (2002).
- [42] N. Brambilla *et al.* (Quarkonium Working Group Collaboration), [arXiv:hep-ph/0412158](https://arxiv.org/abs/hep-ph/0412158).
- [43] B.-Q. Li and K.-T. Chao, *Commun. Theor. Phys.* **52**, 653 (2009).
- [44] Y. Jia, X.-T. Yang, W.-L. Sang and J. Xu, *J. High Energy Phys.* **06** (2011) 097.
- [45] E. Braaten and Y.-Q. Chen, *Phys. Rev. D* **55**, 2693 (1997).
- [46] J. G. Morfin and W.-K. Tung, *Z. Phys. C* **52**, 13 (1991).
- [47] M. Gluck, E. Reya, and A. Vogt, *Z. Phys. C* **67**, 433 (1995).